12) Hoshi K, et al.: Relationship between acridine orange fluorescence of sperm nuclei and the fertilizing ability of human sperm. Fertil Steril 66: 634-639, 1996.
13) Fernandez J, et al.: The sperm chromatin dispersion test: a simple method for the determination of sperm DNA fragmentation. J. Androl 24: 59-66, 2003.
14) Maleszewski M, et al.: Behavior of transgenic mouse spermatozoa with galline protamine. Biol. Reprod 58: 8-14, 1998.
15) Zhao M, et al.: Transition nuclear proteins are required for normal chromatin condensation and functional sperm development. Genesis 38: 200-213, 2004.
16) Kvist U, et al.: Zinc in sperm chromatin and chromatin stability in fertile and men in barren unions. Scand J Urol Nephrol 22: 1-6, 1988.
17) Shoukir Y, et al.: Blastocyst development from supernumerary embryos after intracytoplasmic sperm injection: a paternal influence? Hum Reprod 13: 1632-1637, 1998.
18) Dumoulin JC, Coonen E, et al.: Comparison of *in-vitro* development of embryos originating from either conventional *in-vitro* fertilization or intracytoplasmic sperm injection. Hum Reprod 15: 402-409, 2000.
19) Griffiths TA, et al.: Embryonic development in vitro is compromised by the ICSI procedure. Hum Reprod 15: 1592-1596, 2000.
20) Miller JE, Smith TT: The effect of intracytoplasmic sperm injection and semen parameters on blastocyst development in vitro. Hum Reprod 16: 918-924, 2001.
21) Bungum M, et al.: Day 3 versus day 5 embryo transfer: a prospective randomized study. RBM Online 7: 98-104, 2003.
22) Hsieh YY, et al.: Routine blastocyst culture and transfer: 201 patients' experience. J Assist Reprod Genet 17: 405-408, 2000.
23) Westphal LM, et al.: Effect of ICSI on subsequent blastocyst development and pregnancy rates. J Assist Reprod Genet 20: 113-116, 2003.
24) Landuyt VL, et al.: Blastocyst formation in in vitro fertilization versus intracytoplasmic sperm injection cycles: influence of the fertilization procedure. Fertil Steril 83: 1397-1403, 2005.
25) Swann K, et al.: The cytosolic sperm factor that triggers Ca2 + oscillations and egg activation in mammals is a novel phospholipase C: PLCzeta. Reproduction 127: 431-439, 2004.
26) Greco E, et al.: Efficient treatment of infertility due to sperm DNA damage by ICSI with testicular spermatozoa. Hum Reprod 20: 226-230, 2004.
27) Menezo YJ, et al.: Antioxidants to reduce sperm DNA fragmentation: an unexpected adverse effect. RBM Online 14: 418-421, 2007.

著者連絡先
(〒329-2763)
栃木県那須塩原市井口537-3
国際医療福祉大学病院リプロダクションセンター
片寄治男

BIOLOGY OF REPRODUCTION 80, 235–242 (2009)
Published online before print 5 November 2008.
DOI 10.1095/biolreprod.108.072736

Genetic Loss of *Faah* Compromises Male Fertility in Mice[1]

Xiaofei Sun,[3] Haibin Wang,[4] Masaru Okabe,[6] Kenneth Mackie,[7] Philip J. Kingsley,[3] Lawrence J. Marnett,[3] Benjamin F. Cravatt,[8] and Sudhansu K. Dey[2,3,4,5]

Departments of Pharmacology,[3] Pediatrics,[4] and Cell and Developmental Biology,[5] Division of Reproductive and Developmental Biology, Vanderbilt University Medical Center, Nashville, Tennessee 37232
Genome Information Research Center,[6] Research Institute for Microbial Diseases, Osaka University, Osaka 565-0871, Japan
Department of Psychological and Brain Sciences and the Gill Center for Biomolecular Science,[7] Indiana University, Bloomington, Indiana 47405
The Skaggs Institute for Chemical Biology and Departments of Cell Biology and Chemistry,[8] Scripps Research Institute, La Jolla, California 92037

ABSTRACT

Marijuana is the most commonly used illicit drug. Although there is some indication that reproductive functions in males are impaired in chronic marijuana users, the genetic evidence and underlying causes remain largely unknown. Herein we show that genetic loss of *Faah*, which encodes fatty acid amide hydrolase (FAAH), results in elevated levels of anandamide, an endocannabinoid, in the male reproductive system, leading to compromised fertilizing capacity of sperm. This defect is rescued by superimposing deletion of cannabinoid receptor 1 (*Cnr1*). Retention of *Faah*$^{-/-}$ sperm on the egg zona pellucida provides evidence that the capacity of sperm to penetrate the zona barrier is hampered by elevated anandamide levels. Collectively, the results show that aberrant endocannabinoid signaling via CNR1 impairs normal sperm function. Besides unveiling a new regulatory mechanism of sperm function, this study has clinical significance in male fertility.

anandamide, CNR1, FAAH, male fertility, mouse, sperm, sperm capacitation, sperm motility and transport

INTRODUCTION

There is some evidence that male fertility in humans is negatively regulated by long-term exposure to marijuana extracts (reviewed by Wang et al. [1]). The major psychoactive component of marijuana is Δ^9-tetrahydrocannabinol (THC). Although in vitro experiments have shown that THC exerts adverse effects on sperm function (reviewed by Rossato et al. [2]), there is no in vivo or genetic evidence that cannabinoids impair male fertility. After THC was identified in 1964 [3], research on cannabinoids exploded with the discovery and cloning of two G protein-coupled cannabinoid receptors, brain-type *Cnr1* encoding CNR1 [4, 5] and spleen-type *Cnr2* encoding CNR2 [6]. Around the same time, several endogenous lipid molecules targeting CNR1 and CNR2 were identified, collectively called endocannabinoids. Two of the most studied endocannabinoids are *N*-arachidonoylethanolamide (known as anandamide) and 2-arachidonoylglycerol (2-AG) [7–9]. Anandamide levels are regulated by a balance between the rates of its synthesis and degradation. Anandamide was thought to be produced primarily from *N*-arachidonoylphosphatidylethanolamine (NAPE) by NAPE-hydrolyzing phospholipase D (NAPEPLD) [10]. However, genetic investigations in NAPEPLD-deficient mice [11] and recent identification of other anandamide synthetic pathways [12, 13] demonstrate that regulation of anandamide synthesis is more complex than previously thought. Anandamide is degraded to ethanolamine and arachidonic acid by a membrane-bound fatty acid amide hydrolase (FAAH) [14, 15]. Although FAAH can hydrolyze other endocannabinoids, including 2-AG [16], investigations in *Faah*$^{-/-}$ mice show that FAAH has a major role in regulating the magnitude and duration of anandamide signaling [12, 17].

Sperm undergo a long journey to acquire fertilization capacity [18–20]. Through the process of spermatogenesis, spermatogonia differentiate into highly polarized sperm, which then undergo maturation in the epididymis before capacitation, acquiring motility in the female reproductive tract. After traveling through the uterine lumen and reaching ovulated eggs in the oviduct ampulla, capacitated sperm navigate through cumulus cells surrounding the egg to contact the zona pellucida, the outermost membrane of the egg. On binding to the zona, sperm undergo a Ca^{++}-dependent exocytotic event known as the acrosome reaction, which is essential for their zona penetration and homing into the perivitelline space. After a sperm binds to an egg plasma membrane, the two gametes unite, resulting in egg activation, pronuclear formation, and syngamy. Each step in the process is essential for successful fertilization.

There are reports that endocannabinoids and their receptors are present in the testis and sperm of invertebrates and vertebrates, including sea urchins, frogs, rats, mice, boars, and humans [21]. This conserved expression across species suggests that endocannabinoid signaling has important roles in male reproduction. In vitro studies also showed that endocannabinoid signaling inhibits capacitation of boar sperm in a cAMP-dependent pathway and prevents the acrosome reaction [22] and that anandamide reduces human sperm motility by quenching mitochondrial activity [21]. However, there is no in vivo genetic

[1]Supported by grants DA06668, HD12304, DA11322, DA21696, and P01-CA-77839 from the National Institutes of Health. S.K. Dey is recipient of Method to Extend Research in Time Awards from the National Institute on Drug Abuse and the Eunice Kennedy Shriver National Institute of Child Health and Human Development.
[2]Correspondence and current address: Sudhansu K. Dey, Cincinnati Children's Hospital Medical Center, Cincinnati, OH 45229-3039. FAX: 513 8031160; e-mail: sk.dey@cchmc.org

Received: 13 August 2008.
First decision: 16 September 2008.
Accepted: 29 October 2008.

eISSN: 1259-7268 http://www.biolreprod.org
ISSN: 0006-3363

evidence of endocannabinoid signaling affecting male reproductive functions, to our knowledge.

In this study, we used gene-targeted mice for *Faah* to mimic the conditions of long-term exposure to marijuana. We explored roles of cannabinoid and endocannabinoid signaling in male fertility.

MATERIALS AND METHODS

Mice

Targeted deletion of *Faah*, *Cnr1*, or *Cnr2* in mice (129/SvJ-C57BL/6J) has been previously described [17, 23, 24]. Double mutants for *Faah/Cnr1* or *Faah/Cnr2* were generated using appropriate breeding strategies. Adult wild-type (WT), $Faah^{-/-}$, $Faah^{-/-}/Cnr1^{-/-}$, and $Faah^{-/-}/Cnr2^{-/-}$ mice were housed at an institutional animal care facility according to National Institutes of Health and institutional guidelines. Experiments were conducted on mice between 3 and 4 mo of age. Testes and epididymis from $Faah^{-/-}$ and WT males were processed for anandamide measurement and in situ hybridization.

Western Blotting

Tissue samples were homogenized in lysis buffer (150 mmol/L of NaCl, 1% nonionic detergent, 0.5% deoxycholate, 0.1% SDS, and 50 mmol/L Tris [pH 8]) containing protease and phosphatase inhibitors. The lysates were centrifuged at 9880 × *g* for 10 min at 4°C. Supernatants (25 μg) were boiled for 5 min in SDS sample buffer. Samples were run on 10% SDS-PAGE gels under reducing conditions and transferred onto nitrocellulose membranes. Membranes were blocked with 10% carnation milk in Tris-buffered saline with 0.1 Tween-20) and probed with antibodies against mouse FAAH (1:1000; custom made by the laboratory of Cravatt et al. [17], CNR1 (1:2000) [25], CNR2 (1:250; Cayman), and β-actin (1:100; Santa Cruz Biotechnology) overnight at 4°C. After thorough washings, blots were incubated in peroxidase-conjugated donkey/anti-goat IgG (1:2000) or donkey/anti-rabbit IgG (1:2000; Jackson/ImmunoResearch), followed by washings. Protein signals were detected using chemiluminescent reagents (Amersham).

Immunohistochemistry

Immunostaining in Bouin solution-fixed paraffin-embedded sections (6 μm) was performed using antibodies specific to FAAH (1:200) [17], CNR1 (1:200) [25], or CNR2 (1:250; Cayman) following antigen retrieval in citrate buffer (pH 6.0) for 10 min in an autoclave. A Histostain-Plus (DAB) kit (Zymed) was used to visualize the antigen. Reddish brown deposits indicate sites of positive immunostaining.

Immunofluorescence

Sperm were isolated from the epididymis of mature WT males and thoroughly washed in PBS. Sperm were fixed with 1% formaldehyde at room temperature for 15 min. After blocking in 1% BSA/PBS containing 0.05% Tween-20, sperm were incubated with CNR1 antibody (1:200; ~500 ng/ml of IgG) [25] with or without blocking peptide overnight at 4°C. After thorough washings, secondary antibodies conjugated with Cy3 (Jackson/Immuno-Research) were used to detect immunofluorescence signaling. SYTO13 green fluorescence dye (Invitrogen) was used for nuclear staining.

Anandamide Assay

Testis and sperm (100 mg) were pooled separately from five WT or $Faah^{-/-}$ mice in each group (n = 3–6) and were assayed for anandamide as previously described [26]. Briefly, the preweighed samples were homogenized in ethyl acetate with 0.5% acetic acid. Immediately before homogenization, $^2H_8$-labeled anandamide was added as an internal standard to a mortar. The homogenate was centrifuged, and the supernatant was dried, reconstituted in chloroform, and purified on a silica-based solid-phase extraction cartridge. The eluent was dried, reconstituted in 1:8 of aqueous silver acetate-methanolic silver acetate, and analyzed by reverse-phase positive-ion electrospray ionization-HPLC-tandem mass spectrometry. Quantification was performed by stable isotope dilution against the octadeuterated internal standard.

In Situ Hybridization

Frozen sections (12 μm) were hybridized with ^{35}S-labeled cRNA probes for mouse *Cnr1* or *Cnr2* as described previously [27]. Sections hybridized with sense probes served as negative controls and showed no positive signals.

In Vitro Fertilization

In vitro fertilization (IVF) was performed as previously described [28]. Briefly, WT females were superovulated by intraperitoneal injections of 5 IU of eCG (Sigma), followed by injections of 5 IU of hCG (Sigma) 48 h later. Cumulus-oocyte complexes were collected from the oviduct ampulla 12–14 h after hCG injection and placed in 100-μl droplets of human tubal fluid (HTF) medium (Chemicon). In most IVF experiments, zona-intact eggs were used. In some IVF experiments, zona-free eggs were used. Cumulus-oocyte complexes were treated with hyaluronidase (Sigma), and cumulus-free eggs were then exposed to acidic Tyrode solution and passed through a pipette several times until zona pellucidae were dissolved. Eggs were washed three times in HTF medium and incubated longer than 1 h to allow surface proteins to recover [29]. Sperm were collected from the cauda of the epididymis and placed into 400 ml of HTF medium to allow capacitation for 2.5 h in a humidified 5% CO_2 incubator at 37°C. Sperm (~1.2–1.5 × 10^6 sperm/ml) were then coincubated with eggs to allow fertilization. After 6 h, sperm were removed, and putative zygotes were placed in 200-μl droplets of potassium simplex optimized medium (Chemicon) and incubated in a humidified 5% CO_2 incubator at 37°C. The cleavage rate (two-cell stage) after 24 h was used as an index of fertilization. Formation of blastocysts at 120 h indicated developmental potential of fertilized embryos.

Evaluation of Sperm-Zona Binding in IVF

After sperm were incubated with eggs for 2 h in IVF experiments, eggs were removed. Attached sperm were stained with propidium iodide and fluorescein isothiocyanate (FITC)-conjugated antibody specific to Izumo protein, generated in the laboratory of Inoue et al. [30].

Analysis of the Acrosome Reaction by Flow Cytometry

Wild-type and $Faah^{-/-}$ caudal sperm were incubated in HTF medium with anti-Izumo antibody conjugated with FITC to monitor spontaneous acrosome reaction by flow cytometry at 30-min intervals for up to 3 h. Sperm were stained with propidium iodide (10 μg/ml) 2 min before flow cytometry analysis. Viable sperm were selected by propidium iodide staining, while acrosome-reacted sperm were identified by anti-Izumo antibody staining [30].

Evaluation of Sperm Motility

After capacitation for 30 and 90 min, 20 μl of media containing sperm (2 × 10^6 sperm/ml) was placed on a prewarmed slide under a coverslip. Sperm motility was recorded in 12 frames/sec for 20 sec at a resolution of 640 × 512 pixels. The total travel distance and linear travel distance (linear distance from the starting point to the end point) and the travel time were measured using the Nikon Nis-elements object tracking function. The curvilinear velocity was calculated from the total distance traveled divided by the travel time. The linear velocity was calculated from the linear travel distance divided by the travel time, whereas linearity was calculated from the linear velocity divided by the curvilinear velocity.

RESULTS

$Faah^{-/-}$ Males Have Compromised Fertility

We have previously shown that FAAH is a key metabolic regulator of anandamide levels in mice [17] and that FAAH deficiency results in higher anandamide levels in the female reproductive tract, impairing normal oviductal embryo transport and embryo development [12]. In the course of these studies, analysis of breeding results showed that litter sizes generated by mating WT females with $Faah^{-/-}$ males are 13% smaller than those generated by mating WT females with WT males (Table 1). These results suggested that FAAH deficiency compromises male fertility. This is further evident from our findings of significantly reduced litter sizes generated by mating $Faah^{-/-}$ females with $Faah^{-/-}$ males compared with those generated by mating $Faah^{-/-}$ females with WT males. These breeding results prompted us to further examine fertility of $Faah^{-/-}$ males. We used WT females mated with $Faah^{-/-}$ or WT males. Females were killed on the morning of Day 2 of pregnancy, and oviducts were flushed to record fertilized (two-cell embryos) and

TABLE 1. Reproductive performance of $Faah^{-/-}$ males.

Genotype		No. of litters examined*	Average litter size (mean ± SEM)
Female	Male		
WT	WT	30	8.1 ± 0.4
	$Faah^{-/-}$	23	7.0 ± 0.4†
$Faah^{-/-}$	WT	21	6.3 ± 0.2
	$Faah^{-/-}$	39	4.1 ± 0.3‡

* Litters were sired by different males.
† $P = 0.06$; unpaired *t*-test between litters from WT female × $Faah^{-/-}$ male crossings and those from WT female × WT male crossings.
‡ $P < 0.001$; unpaired *t*-test between litters from $Faah^{-/-}$ female × $Faah^{-/-}$ male crossings and those from $Faah^{-/-}$ female × WT male crossings.

unfertilized eggs. We observed that WT females mated with $Faah^{-/-}$ males have significantly fewer fertilized eggs compared with those recovered from WT females mated with WT males. In addition, fewer WT females yielded fertilized egg (Fig. 1). These data corroborate the breeding data that FAAH deficiency impairs male fertility. Collectively, our findings show that $Faah^{-/-}$ sperm underperform even in the WT female reproductive tract and that function of null sperm is further compromised in the $Faah^{-/-}$ female reproductive tract. These observations provide evidence that paternal FAAH deficiency is a cause for compromised fertility.

Endocannabinoid Signaling Is Present in the Male Reproductive System

The extent and duration of anandamide signaling via CNR1 or CNR2 are mainly regulated by FAAH [17]. Therefore, we examined the expression of CNR1, CNR2, and FAAH in the testis and epididymis to study potential roles of anandamide in regulating male fertility. Western blotting analysis showed that FAAH, CNR1, and CNR2 are present in the testis and epididymis of WT mice (Fig. 2a). We next examined cell-specific localization of FAAH and cannabinoid receptors in the testis and epididymis of WT mice by immunohistochemistry (Fig. 2b). While CNR1 was present in Leydig cells and epididymal epithelial cell surfaces, testicular spermatocytes and spermatids showed modest positive staining. In contrast, CNR2 was localized in spermatocytes and Sertoli cells encircling spermatocytes and spermatids in the testis. In the epididymis, epithelial cell surfaces demonstrated CNR2 immunostaining, whereas signals were undetectable in interstitial cells. FAAH was present in spermatocytes and spermatids, while spermatogonia had little or no positive signal. Sertoli cells and Leydig cells also showed positive staining of FAAH. The localization of FAAH was evident on cell surfaces of the epididymal epithelium. The antibody specificity was confirmed using $Faah^{-/-}$ tissues (Supplemental Figure 1 available online at www.biolreprod.org). The presence of FAAH on the testis and epididymis suggests that endocannabinoid levels are tightly regulated by FAAH in these tissues.

The presence of CNR1 and CNR2 on sperm was also examined by immunofluorescence. As shown in Figure 2c, CNR1 immunofluorescence is primarily noted in anterior regions of sperm heads, the site of the acrosomal sac, but also in the midpiece. CNR1 is undetectable in the principal piece and endpiece of sperm tails. Sperm incubated with CNR1 antibody preabsorbed with an antigenic peptide showed that, while the signal in the anterior region of sperm heads is specific, the signal is nonspecific in the midpiece. CNR2 was undetectable in sperm (Supplemental Figure 2 available online at www.biolreprod.org). Our findings of the presence of FAAH, CNR1, and CNR2 in the testis and epididymis and the presence

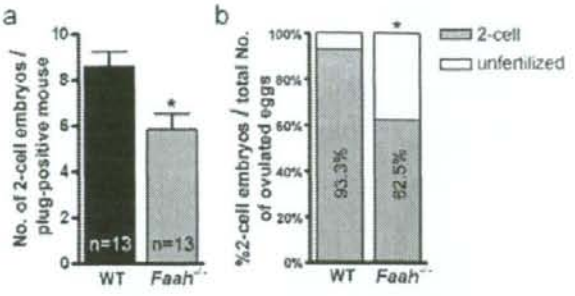

FIG. 1. FAAH deficiency impairs sperm fertility. **a**) Number of two-cell embryos per plug-positive WT females mated with WT or $Faah^{-/-}$ males. Numbers of plug-positive mice used are shown within the bars (* $P < 0.05$, unpaired Student *t*-test). **b**) Percentage of two-cell embryos and unfertilized eggs retrieved from the same groups. Thirteen mice are used in each group (* $P < 0.01$, Chi-square test).

of FAAH and CNR1 in sperm suggest that endocannabinoid signaling has a role in spermatogenesis and sperm maturation.

FAAH Deficiency Elevates Anandamide Levels in the Testis and Epididymis

To provide genetic evidence for function of FAAH in the male reproductive system, we measured anandamide and 2-AG levels in the testis and epididymis of WT and $Faah^{-/-}$ mice using reverse-phase HPLC-tandem mass spectrometry. As shown in Figure 3a, testis and epididymis from $Faah^{-/-}$ mice had significantly increased anandamide levels, suggesting that FAAH is a primary enzyme that regulates anandamide turnover in these tissues. Higher testicular anandamide levels in $Faah^{-/-}$ males corroborate our previous observation [31]. However, levels of 2-AG in the testis and epididymis were comparable between $Faah^{-/-}$ and WT males (Fig. 3a). These results are consistent with our previous data in the uterus showing unaltered 2-AG levels in the absence of FAAH [12].

Higher anandamide levels in the $Faah^{-/-}$ testis and epididymis prompted us to speculate that reduced fertility in these males is due to persistent or elevated endocannabinoid signaling. However, it is possible that there is a negative feedback loop to downregulate the expression of cannabinoid receptors to counter the consequence of high anandamide levels. To address this possibility, we examined the status of cannabinoid receptors in the testis and epididymis of WT and $Faah^{-/-}$ mice by Western blotting. As shown in Figure 3b, levels of CNR1 and CNR2 protein in these tissues were comparable between $Faah^{-/-}$ and WT males. These results suggest that higher anandamide levels do not appreciably downregulate CNR1 or CNR2 expression. To further confirm that expression of CNR1 and CNR2 is not altered in $Faah^{-/-}$ males, in situ hybridization and immunohistochemistry were performed. Expression patterns of CNR1 and CNR2 were similar in WT and $Faah^{-/-}$ epididymis (data not shown). Collectively, the data suggest that the status of cannabinoid receptors is not altered by higher anandamide levels and that heightened signaling via CNR1 or CNR2 occurs in the presence of increased anandamide levels.

FAAH Deficiency Impairs Sperm Fertilizing Capacity

Our in vivo breeding data led us to speculate that higher anandamide levels in males lacking FAAH results in their reduced fertility. To examine this, we first compared histology of

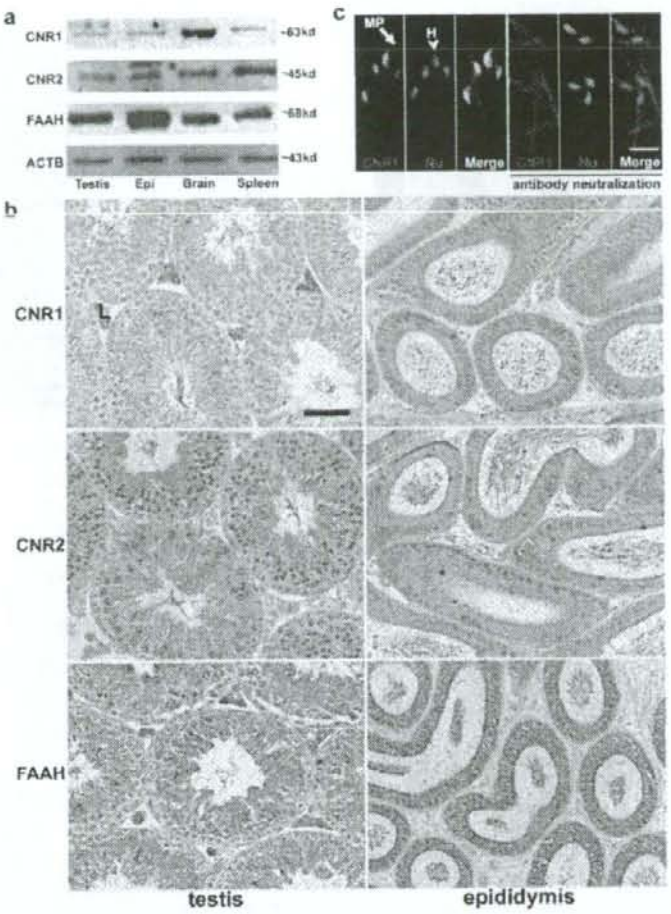

FIG. 2. FAAH and cannabinoid receptors are expressed in the male reproductive tract. **a**) Western blotting of CNR1, CNR2, and FAAH in the WT testis and epididymis. Brain tissue extracts served as positive controls for CNR1 and FAAH, while spleen tissue samples served as positive controls for CNR2. β-Actin (ACTB) is a loading control. Epi, epididymis. **b**) Immunolocalization of CNR1, CNR2, and FAAH in the testis and epididymis. L, Leydig cells. Bar = 50 μm. **c**) CNR1 immunostaining (red) in sperm (left three panels) and in sperm exposed to CNR1 antibody preabsorbed with an antigenic peptide (right three panels). In each group, CNR1 staining, nuclear staining, and merged pictures are shown from left to right. Nuclei were counterstained with SYTO13 (green). MP (arrow), sperm midpiece; H (arrowhead), sperm head; Nu, nuclear. Bar = 10 μm.

the testis and epididymis, as well as sperm morphology, between *Faah*$^{-/-}$ and WT males at the age of 3–4 mo. To our surprise, no apparent histological abnormalities were observed in these tissues missing *Faah* (Supplemental Figure 3 available online at www.biolreprod.org). We next explored whether FAAH deficiency in males impairs the fertilizing capacity of sperm by performing IVF experiments using *Faah*$^{-/-}$ or WT sperm with WT eggs. Sperm retrieved from the caudal epididymis were subjected to capacitation in vitro for 2 h before placing them with eggs in culture. The fertilization rate was calculated by counting the number of two-cell embryos developed on the second day after IVF. As summarized in Table 2, sperm retrieved from WT males showed a 75% fertilization rate, with 97% of two-cell embryos developing to blastocysts (evaluated on the fifth day of culture). In contrast, *Faah*$^{-/-}$ sperm showed a remarkably reduced fertilization rate (42%), although development of fertilized eggs into blastocysts was comparable (89%) to that in WT animals (97%). These results suggest that the fertilizing capacity of *Faah*$^{-/-}$ sperm is compromised because of impairment in the male reproductive tract before ejaculation.

Deletion of Cnr1 *Reverses Impaired Fertilizing Capacity of* Faah$^{-/-}$ *Sperm*

Sustained higher anandamide levels in the male reproductive tract lacking FAAH are capable of exerting endocanna-

TABLE 2. Higher anandamide levels impair sperm fertilizing capacity in vitro via CNR1.

Genotypes	No. of eggs used for IVF	IVF rate		Development	
		Percentage	No. of 2-cell embryos/ total no. of eggs used	Percentage	No. of blastocysts/ total no. of 2-cell embryos used
WT	624	75	466/624	97	450/466
Faah$^{-/-}$	528	42*	221/528*	89	197/221
Faah$^{-/-}$/*Cnr1*$^{-/-}$	177	70	124/177	93	115/124
Faah$^{-/-}$/*Cnr2*$^{-/-}$	118	11*	13/118*	84.6	11/13

* $P < 0.01$; chi-square analysis.

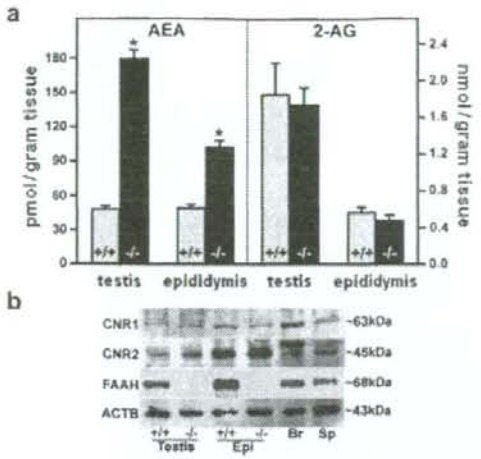

FIG. 3. FAAH deficiency elevates anandamide levels. **a**) Anandamide (AEA) levels, but not 2-AG levels, in *Faah*$^{-/-}$ testis and epididymis were higher than those in WT males (n = 10; * $P < 0.05$, unpaired Student *t*-test). **b**) Western blotting of CNR1, CNR2, and FAAH in the testis and epididymis of WT and *Faah*$^{-/-}$ males. Brain and spleen samples served as positive controls, while β-actin (ACTB) served as a loading control. Epi, epididymis; Br, brain; Sp, spleen.

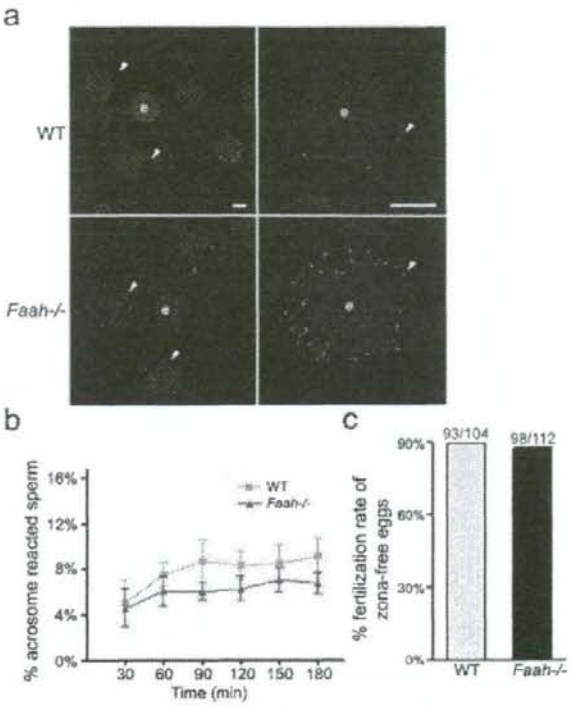

FIG. 4. Zona-penetrating capacity of *Faah*$^{-/-}$ sperm is inferior. **a**) Sperm-egg interactions using zona-intact WT eggs. After 2 h of incubation with eggs, *Faah*$^{-/-}$ sperm were still attached to zona pellucidae. Arrowhead, sperm on the zona-intact egg surface; e, egg. Bar = 40 μm. **b**) Spontaneous acrosome reaction as assessed by flow cytometry. The rate (%) of acrosome-reacted WT and *Faah*$^{-/-}$ sperm at each time point was analyzed by flow cytometry as described in *Materials and Methods*, and no statistically significant difference was noted between the two groups as analyzed by Student *t*-test. **c**) The IVF rates of zona-free WT eggs fertilized by WT or *Faah*$^{-/-}$ sperm. Numbers above the bars indicate the number of fertilized eggs/total zona-free eggs used for IVF.

binoid signaling through CNR1, CNR2, or both. To address this, we generated *Faah*$^{-/-}$/*Cnr1*$^{-/-}$ and *Faah*$^{-/-}$/*Cnr2*$^{-/-}$ double-mutant mice. We again performed IVF using sperm retrieved from *Faah*$^{-/-}$/*Cnr1*$^{-/-}$ or *Faah*$^{-/-}$/*Cnr2*$^{-/-}$ males with eggs isolated from WT females. As summarized in Table 2, sperm isolated from *Faah*$^{-/-}$/*Cnr1*$^{-/-}$ males exhibited a 70% fertilization rate, with 93% of fertilized eggs developing to the blastocyst stage, but sperm isolated from *Faah*$^{-/-}$/*Cnr2*$^{-/-}$ males showed a remarkably low fertilization rate (11%). These data show that, in the absence of CNR1, *Faah*$^{-/-}$ sperm escape the deleterious effects of higher anandamide levels. The inferior fertilizing capacity of *Faah*$^{-/-}$/*Cnr2*$^{-/-}$ sperm exceeded that of *Faah*$^{-/-}$ sperm. The results provide genetic evidence that higher anandamide levels work through CNR1 in the *Faah*$^{-/-}$ male reproductive tract to impair sperm fertilizing capacity.

Faah$^{-/-}$ *Sperm Have Poor Zona-Penetrating Ability*

Our next objective was to see which step in the fertilization process is impaired in *Faah*$^{-/-}$ sperm. We first examined whether *Faah*$^{-/-}$ sperm can adhere to zona pellucidae and, if so, whether they can undergo the acrosome reaction. Izumo, a recently discovered protein, is absent from plasma membranes of acrosome-intact sperm [30]. Following the acrosome reaction, Izumo is exposed and participates in sperm-egg fusion. Therefore, only acrosome-reacted sperm are stained by Izumo antibody.

Wild-type or *Faah*$^{-/-}$ sperm were incubated with WT eggs for 2 h and then stained with propidium iodide to label cell nuclei. After 2 h of incubation, most WT sperm detached from the zona surface (Fig. 4a), whereas numerous *Faah*$^{-/-}$ sperm were still attached to the zona. Even after several washings, *Faah*$^{-/-}$ sperm remained adherent to the zona, indicating good binding of *Faah*$^{-/-}$ sperm to the zona. These results suggested that most eggs were fertilized by WT sperm but that eggs incubated with *Faah*$^{-/-}$ sperm were still unfertilized. We then stained the sperm attached to eggs with Izumo antibody. Many *Faah*$^{-/-}$ sperm remaining on the zona surface showed positive signal by Izumo antibody (Supplemental Figure 4 available online at www.biolreprod.org), indicating that they underwent the acrosome reaction. To further confirm that *Faah*$^{-/-}$ sperm undergo normal acrosome reaction, we examined the spontaneous acrosome reaction rate of *Faah*$^{-/-}$ sperm. The acrosome reaction, which occurs during sperm penetration through the zona, can also occur spontaneously without binding to the zona. Analysis of spontaneous acrosome reaction is used to assess the fertilizing ability of human [32] and mouse [33] sperm. We compared the status and time course of spontaneous acrosome reaction of WT and *Faah*$^{-/-}$ sperm in the fertilization medium by flow cytometry. While viable sperm were selected by propidium iodide staining, acrosome-reacted sperm were identified by Izumo staining. As shown in Figure 4b, the percentage of acrosome-reacted *Faah*$^{-/-}$ sperm is somewhat lower than that of acrosome-reacted WT sperm, but the difference is not statistically significant. Collectively, these data suggest that *Faah*$^{-/-}$ sperm can bind to the zona and undergo the acrosome reaction but still have difficulty in fertilizing eggs.

The acrosome reaction is not the only prerequisite for zona penetration. Sperm motility and acrosomal release of proteases are also involved in this process [20]. To examine whether *Faah*$^{-/-}$ sperm can penetrate the zona successfully, we performed IVF using sperm from *Faah*$^{-/-}$ or WT mice

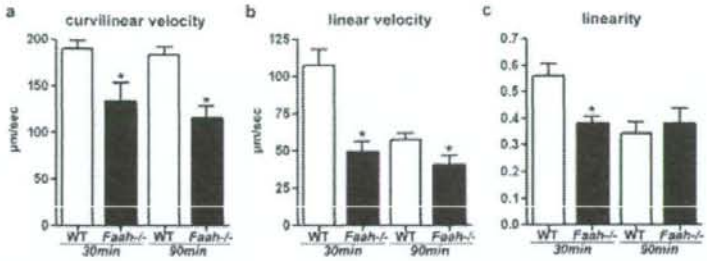

FIG. 5. Motility of *Faah*$^{-/-}$ sperm is inferior. **a**) Curvilinear velocity of WT and *Faah*$^{-/-}$ sperm. Curvilinear velocities of *Faah*$^{-/-}$ sperm were significantly lower than those of WT sperm at 30 and 90 min of capacitation (* $P < 0.01$, unpaired Student *t*-test). **b**) Linear velocity of WT and *Faah*$^{-/-}$ sperm. Linear velocities of *Faah*$^{-/-}$ sperm were significantly lower than those of WT sperm (* $P < 0.05$, unpaired Student *t*-test). **c**) Linearity of WT and *Faah*$^{-/-}$ sperm. Linearity of *Faah*$^{-/-}$ sperm was significantly lower than that of WT sperm at 30 min of capacitation (* $P < 0.05$, unpaired Student *t*-test).

incubated with zona-free WT eggs. To our surprise, *Faah*$^{-/-}$ sperm exhibited fertilizing capacity comparable to that of WT sperm (Fig. 4c), indicating that the zona is a major barrier for normal fertilization by *Faah*$^{-/-}$ sperm.

Sperm Motility Is Attenuated in Faah$^{-/-}$ *Males*

It is generally accepted that robust sperm motility is an important component of normal male fertility [34] and that hyperactivated motility of sperm is correlated with sperm's fertilizing ability of zona-intact eggs [35]. In a low-viscosity medium, motility of hyperactivated sperm is characterized by asymmetrical flagellar bends with large amplitude and curvature, and moving trajectories are irregular and highly curved [36]. We often observed sluggish motility of *Faah*$^{-/-}$ sperm when they were incubated in the capacitation medium. We speculated that the reduced zona-penetrating ability of *Faah*$^{-/-}$ sperm could be due to their reduced motility or hyperactivation. Therefore, we assayed motility of WT and *Faah*$^{-/-}$ sperm after capacitation for 30 and 90 min in vitro. In this measurement, the curvilinear velocity was calculated from the total distance traveled divided by the travel time; this parameter indicates the swimming ability of sperm. The linear velocity was calculated from the distance between the start and end points divided by the travel time. The linearity is the linear velocity-curvilinear velocity ratio; this is an indicator of straightness of sperm movement. The movement of *Faah*$^{-/-}$ sperm was significantly slower than that of WT sperm at 30 and 90 min of incubation in the capacitation medium (Fig. 5a). The movement of WT sperm was primarily straight at 30 min of capacitation, with symmetrical flagellar beats. After 90 min of capacitation, WT sperm showed hyperactivated movement pattern, resulting in reduced linear velocity (Fig. 5b) and linearity (Fig. 5c); the curvilinear velocity was not significantly changed (Fig. 5a). However, *Faah*$^{-/-}$ sperm demonstrated irregular movement from 30 min of capacitation, distinguished by decreased linear velocity and linearity (Fig. 5, b and c). Although their moving trajectories were erratic, the seemingly hyperactivated movement of *Faah*$^{-/-}$ sperm was not the consequence of harder beat of flagellum after capacitation, as the moving speed of *Faah*$^{-/-}$ sperm stayed at low levels. These results show that heightened anandamide signaling in the male reproductive tract compromises motility of *Faah*$^{-/-}$ sperm, leading to reduced zona penetration and fertilization.

DISCUSSION

Emerging evidence shows that endocannabinoid signaling has critical roles in male reproduction. Endocannabinoid signaling is operative in the oviduct, uterus, and embryo, and aberrant endocannabinoid signaling adversely affects oviductal transport of embryos and their development [1]. Consistent with our present findings, endocannabinoids and their receptors were reported to be present in the testis and sperm of invertebrates and vertebrates [21, 22, 37–40]. However, our findings of the endocannabinoid system in different regions along the male reproductive tract suggest that endocannabinoid signaling has diverse physiological functions. In this respect, Sertoli cells exposed to higher anandamide levels were shown to undergo apoptosis [41], and FAAH activity is regulated by FSH in mouse Sertoli cells [42]. In addition, sperm fertility and the acrosome reaction were reported to be adversely affected if exposed in vitro to high anandamide levels [21, 43].

Our experiments were designed to evaluate in vivo effects of sustained higher anandamide levels in the male reproductive tract on various aspects of sperm function. We used *Faah*$^{-/-}$ mice with high anandamide levels as a model system to mimic the conditions of long-term exposure to marijuana use to explore the role of cannabinoid and endocannabinoid signaling in male fertility. Results of our IVF experiments with *Faah*$^{-/-}$ sperm show a resemblance to reduced sperm fertilizing capacity and motility in marijuana users [44–46]. Our findings of compromised fertilizing capacity of *Faah*$^{-/-}$ sperm in vivo and in vitro, as well as their inability to recover in normal capacitating medium, provide strong evidence that functional impairment of sperm exposed to high anandamide levels in vivo persists for a prolonged period or becomes irreversible. Our results are clinically relevant because long-term in vivo exposure to marijuana is implicated in reduced male fertility [44–46].

The use of zona-free eggs in IVF experiments is an established method to study cellular mechanisms of gamete adhesion and fusion [47]. Using this strategy, we have shown that *Faah*$^{-/-}$ sperm are capable of adhering to and fusing with zona-free eggs in a manner similar to that of WT sperm. The fact that the fertilization rate of *Faah*$^{-/-}$ sperm increased from 42% with zona-intact eggs to 90% with zona-free eggs suggests that the zona is a major barrier to *Faah*$^{-/-}$ sperm, as these null sperm display spontaneous acrosome reaction comparable to that of WT sperm based on Izumo staining and flow cytometry analysis. We speculate that factors other than the acrosome reaction weaken the penetrating capacity of sperm through the zona. Sperm motility and acrosomal enzymes are involved in zona penetration [20]. It is possible that contents released from the acrosomal sac lack appropriate protease activity required for penetration or that *Faah*$^{-/-}$ sperm cannot acquire hypermotility following capacitation. Our results suggest that reduced motility is a contributing factor for reduced zona-penetrating ability of *Faah*$^{-/-}$ sperm. However, other factors

such as protease activity may contribute to reduced capacity of sperm for zona penetration. *Faah*$^{-/-}$ sperm show asymmetric flagellar beat at 30 min of capacitation. We do not know whether *Faah*$^{-/-}$ sperm show straightforward moving trajectory before 30 min of capacitation. Although it would be helpful to know the motility of *Faah*$^{-/-}$ sperm immediately after they are placed in the capacitation medium, we were unable to obtain this information because of the time necessary for sperm manipulation and counting.

Reversal of the defects of FAAH deficiency in the absence of CNR1 suggests that anandamide signaling exerts its effects on sperm through CNR1. Because CNR1 is expressed in the testis, epididymis, and sperm, it is unclear where and how CNR1-mediated signaling regulates sperm fertility. Because sperm display CNR1, it is possible that higher anandamide levels directly target sperm to alter their function. Alternatively, heightened signaling via CNR1 in the presence of higher anandamide levels in *Faah*$^{-/-}$ testis and epididymis changes the internal milieu to affect sperm maturation, influencing sperm fertility. Our findings that *Faah*$^{-/-}$/*Cnr2*$^{-/-}$ sperm show much inferior fertilizing capacity than sperm deleted of *Faah*$^{-/-}$ only suggest that anandamide working via CNR2 is important for normal sperm fertility. Alternatively, in the absence of CNR2, higher levels of anandamide are exclusively available to CNR1, further enhancing its adverse effects on sperm function. The latter speculation seems more probable because homozygous crossings of *Cnr2*$^{-/-}$ mice have an average litter size of about seven, whereas homozygous crossings of *Faah*$^{-/-}$/*Cnr2*$^{-/-}$ mice produce an average of four pups per litter. Although breeding data are more confounded by maternal factors than IVF results, this observation suggests that CNR2 has limited roles in sperm function under physiological anandamide levels.

The present investigation has physiological significance because sperm in *Faah*$^{-/-}$ mice and those in chronic marijuana users are subjected to enhanced cannabinoid and endocannabinoid signaling. Beneficial effects of anandamide in neurodegeneration, cancer, pain, and anxiety [48–51] have prompted heightened interest in and effort to develop FAAH inhibitors as novel therapeutic drugs. Therefore, adverse effects of anandamide should be carefully weighed against its beneficial effects. This study provides insights into male fertility regulation by endocannabinoid signaling and may shed light on improving male fertility.

ACKNOWLEDGMENTS

The authors thank Susanne Tranguch for her critical reading of the manuscript and Jiyoung Hong for her technical help.

REFERENCES

1. Wang H, Dey SK, Maccarrone M. Jekyll and Hyde: two faces of cannabinoid signaling in male and female fertility. Endocr Rev 2006; 27: 427–448.
2. Rossato M, Pagano C, Vettor R. The cannabinoid system and male reproductive functions. J Neuroendocrinol 2008; 20(suppl 1):90–93.
3. Gaoni Y, Mechoulam R. Isolation, structure, and partial synthesis of an active constituent of hashish. J Am Chem Soc 1964; 86:1646–1647.
4. Devane WA, Dysarz FA III, Johnson MR, Melvin LS, Howlett AC. Determination and characterization of a cannabinoid receptor in rat brain. Mol Pharmacol 1988; 34:605–613.
5. Matsuda LA, Lolait SJ, Brownstein MJ, Young AC, Bonner TI. Structure of a cannabinoid receptor and functional expression of the cloned cDNA. Nature 1990; 346:561–564.
6. Munro S, Thomas KL, Abu-Shaar M. Molecular characterization of a peripheral receptor for cannabinoids. Nature 1993; 365:61–65.
7. Devane WA, Hanus L, Breuer A, Pertwee RG, Stevenson LA, Griffin G, Gibson D, Mandelbaum A, Etinger A, Mechoulam R. Isolation and structure of a brain constituent that binds to the cannabinoid receptor. Science 1992; 258:1946–1949.
8. Mechoulam R, Ben-Shabat S, Hanus L, Ligumsky M, Kaminski NE, Schatz AR, Gopher A, Almog S, Martin BR, Compton DR, Pertwee RG, Griffin G, et al. Identification of an endogenous 2-monoglyceride, present in canine gut, that binds to cannabinoid receptors. Biochem Pharmacol 1995; 50:83–90.
9. Sugiura T, Kudo N, Ojima T, Mabuchi-Itoh K, Yamashita A, Waku K. Coenzyme A-dependent cleavage of membrane phospholipids in several rat tissues: ATP-independent acyl-CoA synthesis and the generation of lysophospholipids. Biochim Biophys Acta 1995; 1255:167–176.
10. Okamoto Y, Morishita J, Tsuboi K, Tonai T, Ueda N. Molecular characterization of a phospholipase D generating anandamide and its congeners. J Biol Chem 2004; 279:5298–5305.
11. Leung D, Saghatelian A, Simon GM, Cravatt BF. Inactivation of *N*-acyl phosphatidylethanolamine phospholipase D reveals multiple mechanisms for the biosynthesis of endocannabinoids. Biochemistry 2006; 45:4720–4726.
12. Liu J, Wang L, Harvey-White J, Osei-Hyiaman D, Razdan R, Gong Q, Chan AC, Zhou Z, Huang BX, Kim HY, Kunos G. A biosynthetic pathway for anandamide. Proc Natl Acad Sci U S A 2006; 103:13345–13350.
13. Simon GM, Cravatt BF. Endocannabinoid biosynthesis proceeding through glycerophospho-*N*-acyl ethanolamine and a role for alpha/beta-hydrolase 4 in this pathway. J Biol Chem 2006; 281:26465–26472.
14. Cravatt BF, Giang DK, Mayfield SP, Boger DL, Lerner RA, Gilula NB. Molecular characterization of an enzyme that degrades neuromodulatory fatty-acid amides. Nature 1996; 384:83–87.
15. Giang DK, Cravatt BF. Molecular characterization of human and mouse fatty acid amide hydrolases. Proc Natl Acad Sci U S A 1997; 94:2238–2242.
16. McKinney MK, Cravatt BF. Structure and function of fatty acid amide hydrolase. Annu Rev Biochem 2005; 74:411–432.
17. Cravatt BF, Demarest K, Patricelli MP, Bracey MH, Giang DK, Martin BR, Lichtman AH. Supersensitivity to anandamide and enhanced endogenous cannabinoid signaling in mice lacking fatty acid amide hydrolase. Proc Natl Acad Sci U S A 2001; 98:9371–9376.
18. Nixon B, Aitken RJ, McLaughlin EA. New insights into the molecular mechanisms of sperm-egg interaction. Cell Mol Life Sci 2007; 64:1805–1823.
19. Okabe M, Cummins JM. Mechanisms of sperm-egg interactions emerging from gene-manipulated animals. Cell Mol Life Sci 2007; 64:1945–1958.
20. Primakoff P, Myles DG. Penetration, adhesion, and fusion in mammalian sperm-egg interaction. Science 2002; 296:2183–2185.
21. Rossato M, Ion Popa F, Ferigo M, Clari G, Foresta C. Human sperm express cannabinoid receptor Cb1, the activation of which inhibits motility, acrosome reaction, and mitochondrial function. J Clin Endocrinol Metab 2005; 90:984–991.
22. Maccarrone M, Barboni B, Paradisi A, Bernabo N, Gasperi V, Pistilli MG, Fezza F, Lucidi P, Mattioli M. Characterization of the endocannabinoid system in boar spermatozoa and implications for sperm capacitation and acrosome reaction. J Cell Sci 2005; 118:4393–4404.
23. Zimmer A, Zimmer AM, Hohmann AG, Herkenham M, Bonner TI. Increased mortality, hypoactivity, and hypoalgesia in cannabinoid CB1 receptor knockout mice. Proc Natl Acad Sci U S A 1999; 96:5780–5785.
24. Jarai Z, Wagner JA, Varga K, Lake KD, Compton DR, Martin BR, Zimmer AM, Bonner TI, Buckley NE, Mezey E, Razdan RK, Zimmer A, et al. Cannabinoid-induced mesenteric vasodilation through an endothelial site distinct from CB1 or CB2 receptors. Proc Natl Acad Sci U S A 1999; 96:14136–14141.
25. Twitchell W, Brown S, Mackie K. Cannabinoids inhibit N- and P/Q-type calcium channels in cultured rat hippocampal neurons. J Neurophysiol 1997; 78:43–50.
26. Wang H, Guo Y, Wang D, Kingsley PJ, Marnett LJ, Das SK, DuBois RN, Dey SK. Aberrant cannabinoid signaling impairs oviductal transport of embryos. Nat Med 2004; 10:1074–1080.
27. Das SK, Wang XN, Paria BC, Damm D, Abraham JA, Klagsbrun M, Andrews GK, Dey SK. Heparin-binding EGF-like growth factor gene is induced in the mouse uterus temporally by the blastocyst solely at the site of its apposition: a possible ligand for interaction with blastocyst EGF-receptor in implantation. Development 1994; 120:1071–1083.
28. Matsumoto H, Ma W, Smalley W, Trzaskos J, Breyer RM, Dey SK. Diversification of cyclooxygenase-2-derived prostaglandins in ovulation and implantation. Biol Reprod 2001; 64:1557–1565.
29. Yamagata K, Nakanishi T, Ikawa M, Yamaguchi R, Moss SB, Okabe M. Sperm from the calmegin-deficient mouse have normal abilities for

binding and fusion to the egg plasma membrane. Dev Biol 2002; 250:348–357.
30. Inoue N, Ikawa M, Isotani A, Okabe M. The immunoglobulin superfamily protein Izumo is required for sperm to fuse with eggs. Nature 2005; 434: 234–238.
31. Cravatt BF, Saghatelian A, Hawkins EG, Clement AB, Bracey MH, Lichtman AH. Functional disassociation of the central and peripheral fatty acid amide signaling systems. Proc Natl Acad Sci U S A 2004; 101: 10821–10826.
32. Ohashi K, Saji F, Kato M, Tsutsui T, Tomiyama T, Tanizawa O. Acrobeads test: a new diagnostic test for assessment of the fertilizing capacity of human spermatozoa. Fertil Steril 1995; 63:625–630.
33. Inoue N, Ikawa M, Nakanishi T, Matsumoto M, Nomura M, Seya T, Okabe M. Disruption of mouse CD46 causes an accelerated spontaneous acrosome reaction in sperm. Mol Cell Biol 2003; 23:2614–2622.
34. Turner RM. Moving to the beat: a review of mammalian sperm motility regulation. Reprod Fertil Dev 2006; 18:25–38.
35. Boatman DE, Robbins RS. Bicarbonate: carbon-dioxide regulation of sperm capacitation, hyperactivated motility, and acrosome reactions. Biol Reprod 1991; 44:806–813.
36. Suarez SS, Katz DF, Owen DH, Andrew JB, Powell RL. Evidence for the function of hyperactivated motility in sperm. Biol Reprod 1991; 44:375–381.
37. Schuel H, Goldstein E, Mechoulam R, Zimmerman AM, Zimmerman S. Anandamide (arachidonylethanolamide), a brain cannabinoid receptor agonist, reduces sperm fertilizing capacity in sea urchins by inhibiting the acrosome reaction. Proc Natl Acad Sci U S A 1994; 91:7678–7682.
38. Sugiura T, Kondo S, Sukagawa A, Tonegawa T, Nakane S, Yamashita A, Waku K. Enzymatic synthesis of anandamide, an endogenous cannabinoid receptor ligand, through *N*-acylphosphatidylethanolamine pathway in testis: involvement of Ca(2+)-dependent transacylase and phosphodiesterase activities. Biochem Biophys Res Commun 1996; 218:113–117.
39. Maccarrone M, Finazzi-Agro A. The endocannabinoid system, anandamide and the regulation of mammalian cell apoptosis. Cell Death Differ 2003; 10:946–955.
40. Wenger T, Ledent C, Csernus V, Gerendai I. The central cannabinoid receptor inactivation suppresses endocrine reproductive functions. Biochem Biophys Res Commun 2001; 284:363–368.
41. Maccarrone M, Cecconi S, Rossi G, Battista N, Pauselli R, Finazzi-Agro A. Anandamide activity and degradation are regulated by early postnatal aging and follicle-stimulating hormone in mouse Sertoli cells. Endocrinology 2003; 144:20–28.
42. Rossi G, Gasperi V, Paro R, Barsacchi D, Cecconi S, Maccarrone M. Follicle-stimulating hormone activates fatty acid amide hydrolase by protein kinase A and aromatase-dependent pathways in mouse primary Sertoli cells. Endocrinology 2007; 148:1431–1439.
43. Schuel H, Burkman LJ, Lippes J, Crickard K, Mahony MC, Giuffrida A, Picone RP, Makriyannis A. Evidence that anandamide-signaling regulates human sperm functions required for fertilization. Mol Reprod Dev 2002; 63:376–387.
44. Kolodny RC, Masters WH, Kolodner RM, Toro G. Depression of plasma testosterone levels after chronic intensive marihuana use. N Engl J Med 1974; 290:872–874.
45. Hembree WC, Nahas GG, Zeidenberg P, Huang HFS. Changes in human spermatozoa associated with high dose marihuana smoking. In: Nahas GG, Paton WDM (eds.), Marihuana: Biological Effects. New York: Oxford; 1979:429–439.
46. Nahas GG, Frick HC, Lattimer JK, Latour C, Harvey D. Pharmacokinetics of THC in brain and testis, male gametotoxicity and premature apoptosis of spermatozoa. Hum Psychopharmacol 2002; 17:103–113.
47. Evans JP. The molecular basis of sperm-oocyte membrane interactions during mammalian fertilization. Hum Reprod Update 2002; 8:297–311.
48. Kathuria S, Gaetani S, Fegley D, Valino F, Duranti A, Tontini A, Mor M, Tarzia G, La Rana G, Calignano A, Giustino A, Tattoli M, et al. Modulation of anxiety through blockade of anandamide hydrolysis. Nat Med 2003; 9:76–81.
49. Lichtman AH, Shelton CC, Advani T, Cravatt BF. Mice lacking fatty acid amide hydrolase exhibit a cannabinoid receptor-mediated phenotypic hypoalgesia. Pain 2004; 109:319–327.
50. Bifulco M, Di Marzo V. Targeting the endocannabinoid system in cancer therapy: a call for further research. Nat Med 2002; 8:547–550.
51. Guzman M. Cannabinoids: potential anticancer agents. Nat Rev Cancer 2003; 3:745–755.

Biochemical and Biophysical Research Communications 377 (2008) 910–914

Contents lists available at ScienceDirect

Biochemical and Biophysical Research Communications

journal homepage: www.elsevier.com/locate/ybbrc

Putative sperm fusion protein IZUMO and the role of *N*-glycosylation

Naokazu Inoue, Masahito Ikawa, Masaru Okabe *

Research Institute for Microbial Diseases, Osaka University, Yamadaoka 3-1, Suita, Osaka 565-0871, Japan

ARTICLE INFO

Article history:
Received 10 October 2008
Available online 24 October 2008

Keywords:
Sperm
Egg
Fusion
Fertilization
N-glycan
Transgenic mouse
Cauda epididymis

ABSTRACT

IZUMO is the mouse sperm protein proven to be essential for fusion with eggs. It contains one immunoglobulin-like domain with a conserved glycosylation site within. In the present paper, we produced transgenic mouse lines expressing unglycosylated IZUMO (N204Q-IZUMO) in *Izumo1* −/− background. The expression of N204Q-IZUMO rescued the infertile phenotype of IZUMO disrupted mice, indicating glycosylation is not essential for fusion-facilitating activity of IZUMO. The N204Q-IZUMO was produced in testis in comparable amounts to wild-type IZUMO, but the amount of N204Q-IZUMO on sperm was significantly decreased by the time sperm reached the cauda epididymis. These data suggest that glycosylation is not essential for the function of IZUMO, but has a role in protecting it from fragmentation in cauda epididymis.

Glycosylation is the most common post-translational modification of proteins, with glycans involved in many key biological processes such as cell adhesion, molecular trafficking and clearance, receptor activation, signal transduction, and endocytosis [1].

The importance of glycans has been demonstrated in reproductive biology. For example, when the enzyme α-mannosidase IIx (MX) is disrupted, spermatogenic cells fail to adhere to Sertoli cells and are prematurely released from the testis, resulting in male infertility [2]. Disruption of the testis-specific, lectin-type molecular chaperone CALMEGIN leads to the disappearance of various glycoproteins from sperm surface and results in male infertility [3–5].

On the other hand, the importance of *O*-linked glycan of the zona component ZP3, which forms a sperm receptor [6], has been reported. This was reinforced by the experiment in which mouse ZP3 gene was replaced by human gene. The result indicated that the peptide sequence of ZP3 is not the crucial factor for species-specific binding of sperm [7]. Moreover, it has been suggested for many years that D(+)-glucosamine, bovine–albumin–glucosamide and D(+)-galactosamide, fucoidan and dextran sulphate have inhibitory effects on sperm–egg fusion [8], but the mechanism of their actions is not clarified.

Recently, we reported IZUMO null sperm cannot fuse with eggs [9]. Since IZUMO is a member of an immunoglobulin superfamily protein and possesses a well-conserved putative *N*-glycosylation site, we examined the role of the glycosylation in IZUMO. For this purpose, we produced transgenic mouse lines that have IZUMO with no *N*-glycosylation site and crossed to the IZUMO disrupted mouse line. The fertilizing ability of these mice with unglycosylated IZUMO was analyzed both *in vitro* and *in vivo* to elucidate the role of glycosylation in IZUMO.

Materials and methods

Animals, cells, and antibodies. IZUMO-null mice were prepared as indicated in our previous paper [9]. BDF1 male and female mice were purchased from SLC. Chinese hamster ovary (CHO) cells were obtained from RIKEN Cell Bank (RIKEN, Saitama, Japan). Anti-IZUMO monoclonal antibody (#125) was previously generated in our laboratory according to the standard method [3]. All of the experiments were performed with the approval of the Animal Care and Use Committee of Osaka University.

Western blotting. Proteins from testis, corpus epididymis and epididymal sperm were solubilized with 1% Triton X-100, 150 mM NaCl, 50 mM Tris–HCl (pH 8.0) and 1% protease inhibitor cocktail (nakalai tesque, Kyoto, Japan), and was centrifuged at 15,000 rpm for 30 min at 4 °C. The supernatants were denatured by boiling for 5 min in the presence of 1% SDS with or without 6% 2-mercaptoethanol, separated by SDS–PAGE, and transferred onto Immobilon-P membranes (Millipore, MA, USA). After blocking with 10% skimmed milk, the blots were incubated with primary antibodies for 2 h and then incubated with horseradish peroxidase-conjugated secondary antibodies for 1 h. Immunoreactive proteins were detected by an ECL Western blotting detection kit (GE Healthcare, Little Chalfont, England).

* Corresponding author. Fax: +81 6 6879 8376.
E-mail address: okabe@gen-info.osaka-u.ac.jp (M. Okabe).

0006-291X/$ - see front matter © 2008 Elsevier Inc. All rights reserved.
doi:10.1016/j.bbrc.2008.10.073

Deglycosylation assay of IZUMO. The methods for analyses using deglycosidase were described previously [10]. Briefly, sperm were solubilized with solubilization buffer containing 1% Triton X-100, 20 mM Tris-maleate (pH 7.4), 1 mM PMSF for *N*-glycosidase F, or 1% Triton X-100, 20 mM sodium citrate (pH 5.9), 1 mM PMSF for Endglycosidase H, or 1% Triton X-100, 20 mM Tris–maleate (pH 6.0), 1 mM PMSF for O-glycosidase. Solubilized proteins were centrituged at 15,000 rpm for 30 min at 4 °C and the supernatants were treated with 250 mU of *N*-glycosidase, or 250 mU of Endglycosidase, or 1 mU of *O*-glycosidase for 16 h at 37 °C. The samples were subjected to SDS–PAGE followed by Western blotting. IZUMO protein was detected with IZUMO polyclonal antibody.

Production of transgenic mice. A construct was prepared in the pBluescript SK II+ plasmid. We designed testis-specific expression construct inserting *Izumo1* cDNA between *Calmegin* promoter and a rabbit β-globin polyadenylation signal. Point mutation (N204Q) was inserted using the QuikChange site-directed mutagenesis system (Stratagene, CA, USA). All constructs were verified by DNA sequencing using an ABI 310 sequencer (Applied Biosystems, CA, USA).

Transgenic mouse lines were produced by injecting 2.3 kb AseI–XhoI DNA fragment into pronuclei of BDF1 × BDF1 fertilized eggs. Offspring carrying the transgene were identified by PCR using Primer A (5′-CCTTCCTGCGGCTTGTTCTCT-3′) and Primer B (5′-GG TCTCAGAACTTTGCTCCCAAACCCTGTA-3′) for wild-type *Izumo1* and *N204Q-Izumo1* cDNA. The endogenous *Izumo1* and their mutated alleles were detected by PCR using Primer C (5′-GGGTT CACTCTCCAGCTACCCCAAACTCAC-3′) and Primer D (5′-CAGAAC CCCGAACCCAGCCTATGCC-3′), and Primer E (5′-GCTTGCCGAATATC ATGGTGGAAAATGGCC-3′) and Primer D, respectively.

Sperm–egg fusion assay. Mouse sperm were collected from cauda epididymides and capacitated *in vitro* for 2 h in 200 μl drop of TYH medium covered with paraffin oil. Female mice (>8-weeks-old) were superovulated with injection of 5 IU of hCG (human chorionic gonadotropin) 48 h after a 5 IU injection of equine chorionic gonadotropin (eCG). The eggs were collected from the oviduct 14 h after the hCG injection. Eggs were placed in a 200 μl drop of TYH medium. After being freed from cumulus cells with 0.01% (w/v) hyaluronidase, the zona pellucida was removed from mouse eggs using a piezo-manipulator as previously reported [11]. The zona-free mouse oocytes were pre-loaded with Hoechst 33342 by incubating them with 1 μg/ml of the dye in TYH for 10 min. After washing, the eggs were incubated with 2×10^5 sperm/ml incubated for 30 min at 37 °C in 5% CO_2, and unbound sperm were washed away. The eggs were observed under a fluorescence microscope (UV excitation light) after fixing with 0.25% glutaraldehyde. This procedure enabled staining of only fused sperm nucleus by transferring the dye into sperm after membrane fusion as in Fig. 2C.

Observation of zona pellucida-penetrated sperm. B6D2F1 females were superovulated by intraperitoneal injection of 5 IU of eCG, followed 48 h later by 5 IU of hCG. Superovulated females were caged together with test males after hCG injection, and the formation of vaginal plug was observed 20 h later. Eggs were collected from the oviduct and placed in a 200 μl drop of TYH medium. After being freed from cumulus cells with 0.01% (w/v) hyaluronidase, these eggs were washed several times by transferring them into fresh medium. Immunostaining was performed by incubating the fertilized eggs with 1 μg/ml #125 Mab for 1 h at 37 °C in 5% CO_2 in 100 μl TYH medium and subsequently secondary antibody staining was done with 10 μg/ml Alexa fluor 546-conjugated anti-rat IgG (Invitrogen, CA, USA) in 100 μl drop of TYH medium for 1 h at 37 °C in 5% CO_2. After repeated washing to observe zona pellucida-penetrated sperm, four small dabs of Vaserine mix (Vaseline: solid paraffin = 9:1) were applied on a slide glass. The eggs were gently pressed with cover glass to flatten them under the stereoscopic microscope, and were then viewed using a fluorescence microscope.

Results

Glycosylation status in IZUMO

IZUMO has four putative *O*-glycosylation sites at the 268th, 274th, 279th and 282nd threonine according to computer analysis using NetOGlyc 3.1 Server (http://www.cbs.dtu.dk/services/NetOGlyc/). However, when we treated IZUMO with *O*-glycosidase, we could not observe any decrease in molecular weight, suggesting IZUMO does not have any *O*-glycans (Fig. 1B). Since IZUMO was also predicted to possess a well-conserved *N*-glycosylation site in the middle of an immunoglobulin-like loop among species (Fig. 1A), we treated mouse sperm IZUMO with two kinds of *N*-glycosidases and examined the change of molecular weight. The molecular weight of Endo

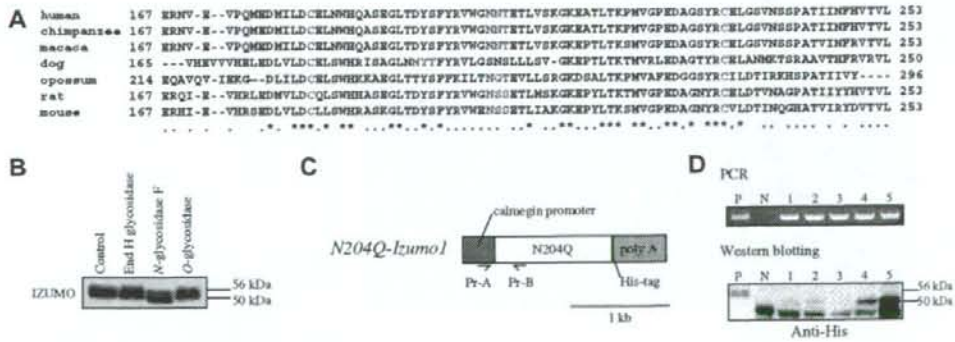

Fig. 1. Deglycosylation study and establishment of N204Q-IZUMO mice. (A) Amino acid sequences of Immunoglobulin-like domain of IZUMO from human, chimpanzee, macaca, dog, opossum, rat, and mouse. A *N*-glycoside link motif and putative cysteine residues that form a disulphide bridge are shown in red and blue, respectively. The similar and identical amino acid residues are shown by a dot and asterisk, respectively. (B) Deglycosylation study of IZUMO. Solubilized sperm proteins (10 μg) were treated with Endo H or *N*- or O-glycosidase. The samples were subjected to SDS–PAGE followed by Western blotting and detected with anti-IZUMO polyclonal antibody under non-reduced conditions. (C) The constructs of transgene to express mouse N204Q-IZUMO were under the control of a *Calmegin* promoter. The locations of a pair of primers (A and B) to clarify the transgene were indicated by arrows. (D) Identification of N204Q-IZUMO-expressing male mice. The upper panel shows 671-bp PCR band using Primer set A and B. The lower panel shows Western blot analysis of testes extracts (50 μg) from transgenic mice. Western blot analysis under reduced conditions was performed by detecting with anti-His tag antibody (Qiagen). The testes extracts from wild-type IZUMO rescue and wild-type were used as a positive and negative control, respectively.

H-treated IZUMO was not altered, but *N*-glycosidase F-treated IZUMO showed higher electrophoretic mobility and the estimated molecular weight changed from approximately 56–50 kDa (Fig. 1B). Since Endo H *N*-glycosidase is reported to hydrolyze only high mannose and some hybrid *N*-glycans, whereas *N*-glycosidase F is reported to cleave most *N*-glycans, including high mannose, hybrid, and complex structures, the digestion results indicate that IZUMO had a complex *N*-glycan structure. Since the stoichiometric molecular mass of IZUMO deduced from its amino acid sequence is 43.5 k, there remains an additional possibility that IZUMO has been modified by some means other than glycosylation, such as phosphorylation or palmitoylation etc.

Establishment of mutated IZUMO expressing mouse line under IZUMO-null background (N204Q-IZUMO)

Since glycan composition is known to be involved in many molecular interaction mechanisms [1], we tried to examine the role of *N*-glycan on IZUMO. Accordingly we produced mouse lines expressing mutated IZUMO by replacing 204th putative *N*-glycosylation site (Asn-X-[Thr/Ser]) aspargine to glutamine by site-directed mutagenesis, and inserted between a testis-specific *Calmegin* promoter and rabbit β-globin polyadenylation signal [4] (Fig. 1C). Since our previous studies showed the addition of His-tag to the carboxy terminal of IZUMO did not affect its function, we performed the above task to make the transgenic protein distinguishable from endogenous IZUMO. After microinjection of the transgene into fertilized eggs and transplantation into pseudopregnant female, we obtained 68 pups and among those, 12 mice were shown to have the transgene by PCR (Fig. 1D; upper panel). Transgenic mouse lines obtained were tested for their expression of mutated IZUMO by Western blot analysis. As illustrated in Fig. 1D, in 4 out of tested 5 transgenic lines, we could detect the production of mutated ~50 kDa IZUMO by anti-His tag antibody. The apparent expression levels of IZUMO in testes of lines #4 and #5 were greater than those of the His-tagged wild-type *Izumo1* transgene that was already shown to rescue the sterility of IZUMO-null male mice [9] (Fig. 1D; lower panel). In the present experiment, lines #4 and #5 were backcrossed to IZUMO-null mice to produce mutant mouse lines that completely lack *N*-glycan of IZUMO (referred to hereafter as N204Q-IZUMO).

The localization of transgenic N204Q-IZUMO and the fertility in male mice

We established N204Q-IZUMO males of #4 and #5 transgenic mouse lines with *Izumo1* −/− background to evaluate the necessity of *N*-glycosylation in IZUMO. Three males from each of the transgenic mouse lines were each caged with three wild-type females and kept for 3 months. Although the litter sizes were smaller compared to the rescued *Izumo1* −/− mice with wild-type IZUMO, the N204Q-IZUMO of both #4 and #5 lines could rescue the infertile sperm back to a fertile state (Fig. 2A). We then performed sperm–

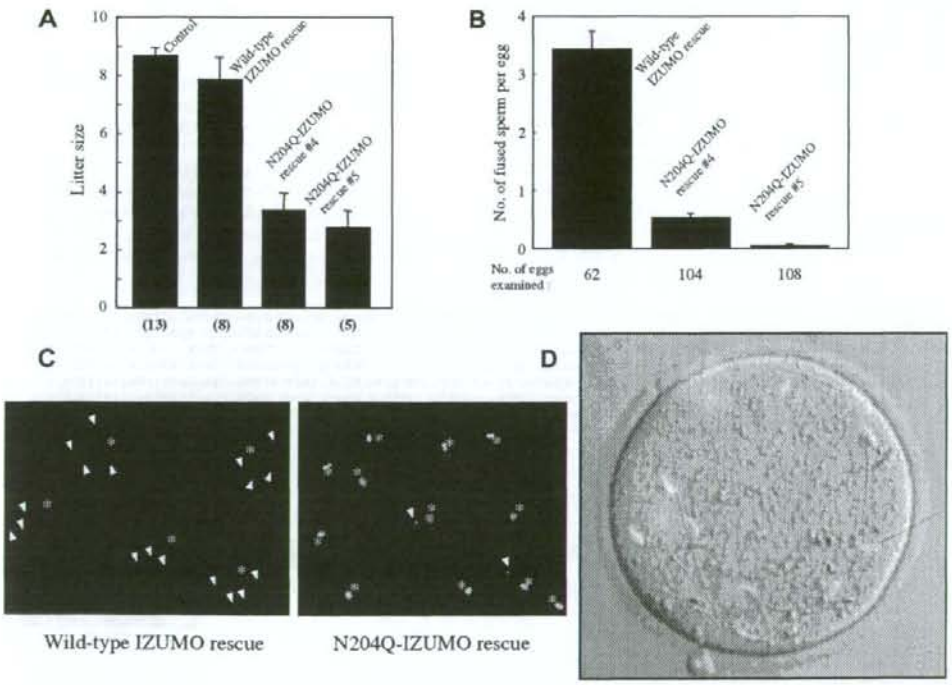

Fig. 2. Fusing ability and subcellular localization of N204Q-IZUMO. (A) Litter size of male mice of control wild-type, and IZUMO-null rescued by wild-type and N204Q-IZUMO (#4, #5 lines) as a transgene. The numbers in parentheses indicate the numbers of mating pairs. Values are presented as means ± standard error of mean (SEM). (B and C) Comparison of the fusing ability of wild-type and N204Q-IZUMO-rescued sperm. Average numbers of fused sperm observed 30 min after insemination ($n = 4$). Values are presented as means ± SEM. Representative photos were shown in C. The arrowheads and asterisks indicate fused sperm and metaphase II-arrested chromosomes, respectively. (D) The localization of N204Q-IZUMO after zona pellucida penetration in naturally acrosome reacted sperm. The migration of N204Q-IZUMO on zona penetrated sperm (acrosome reacted sperm) was normal and seen in the entire head region as observed in wild-type sperm (red signal).

egg fusion assay using zona-free eggs prepared by the piezo-manipulator method [11]. The sperm from both #4 and #5 lines were able to bind to the plasma membrane of eggs as well as to wild-type IZUMO-rescued sperm when observed 30 min after the sperm insemination. The efficiency was low, but sperm from N204Q-IZUMO could fuse with eggs (Fig. 2B and C).

IZUMO is located inside acrosome and exposed on sperm surface only after acrosome reaction. After IZUMO is exposed on the surface, it migrates and spreads across the entire head area including the equatorial segment where sperm–egg fusion takes place [9]. We then examined whether the loss of glycosylation in IZUMO affects the nature of translocation of IZUMO after acrosome reaction. When we stained sperm inside the perivitelline space, N204Q-IZUMO was found to be localized on entire sperm head in the same manner with wild-type IZUMO (Fig. 2D). These data suggest that the absence of *N*-glycan on IZUMO had little or no influence on the transposition of the antigen on sperm surface which accompanied acrosome reaction. However, the staining intensities were dimmer than those of wild-type IZUMO.

Putative function of N-glycan in IZUMO

We previously produced monoclonal antibody (Mab) against mouse IZUMO (#125) [3]. We extracted proteins from testis and sperm from male mice in lines #4 and #5 and analyzed them by Western blot analysis using Mab#125. The N204Q-IZUMO was migrated as a 50 kDa band probably due to the lack of *N*-linked glycan at N204 site. However, in sperm, a severe fragmentation of N204Q-IZUMO was observed while it was not apparent in wild-type IZUMO or testicular N204Q-IZUMO (Fig. 3A). The major fragmented bands were observed at ~30 and 35 kDa area. This fragmentation was not observed in sperm until sperm reached the cauda epididymis (Fig. 3B). It should be noted that the 30 kDa band disappeared when anti-His tag antibody was used, indicating that 35 kDa fragment contains carboxy-terminal His tag, but that the 30 kDa band did not (Fig. 3C).

Although N204Q-IZUMO could rescue the infertile phenotype, the amount of intact N204Q-IZUMO presented on sperm was significantly small compared to wild-type IZUMO in spite of an abundance of N204Q-IZUMO in testis (Fig. 3A). This decrease was

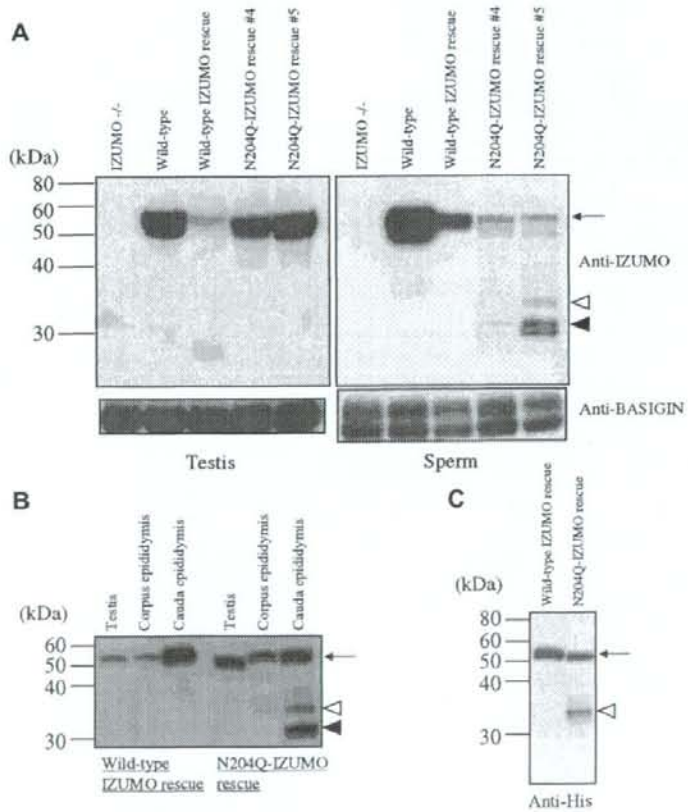

Fig. 3. Fragmentation of N204Q-IZUMO protein in cauda epididymal sperm. (A) N204Q-IZUMO is fragmented by protease in cauda epididymal sperm. Solubilized proteins (30 μg) from testes and sperm were separated by SDS–PAGE in a 10% polyacrylamide gel, and detected with #125 Mab. Immunoglobulin superfamily protein BASIGIN (CD147) was shown in the lower panel as a control. The arrow and filled and unfilled arrowheads are indicated by 50 kDa unglycosylated IZUMO and ~30 and 35 kDa fragmented products, respectively. (B) IZUMO reactivity in testis and epididymis. The 30 μg of proteins from extracts of testis (testicular cell), corpus epididymis (tissue) and sperm from cauda epididymis were separated on a 10% SDS–PAGE and subjected to Western blot analysis. The bolts were incubated with #125 Mab. (C) Western blotting with carboxy terminal antibody. The 30 μg of proteins from cauda epididymal sperm were immunoreacted with anti-His tag antibody. All Western blot analyses were performed under reduced conditions in this figure.

characteristic to N204Q-IZUMO and was not observed in the wild-type IZUMO-rescued mice (Fig. 3A and C).

Discussion

Fragmentation of unglycosylated IZUMO in cauda epididymis

The membranous proteins of sperm are exposed to proteases, and are modified during epididymal transit. For example, testicular angiotensin I-converting enzyme (tACE) is released from the testicular sperm membrane to epididymal fluid when sperm enter the epididymis [12] and this is indispensable for sperm to bind to zona pellucida properly [13].

IZUMO is a membrane protein and is not exposed to the outside of sperm, but is hidden under the plasma membrane before acrosome reaction. Therefore, the fragmentation of unglycosylated IZUMO during epididymal maturation must be caused by acrosomal proteases such as ACROSIN, TESP1, TESP2, PRSS2 and PRSS21, etc. [14–17]. We reported the rise of pH level inside acrosome during the incubation of epididymal sperm in capacitation medium [18]. This pH change could facilitate some enzymes to be activated, but the enzyme that cleaves IZUMO must be activated before capacitation. As far as we know, there are no precedent papers reporting activation of proteases inside acrosome during epididymal maturation. Although the processing of unglycosylated IZUMO is not a physiological phenomenon, the result indicates that some acrosomal enzymes are activated during maturation in epididymis and process membrane proteins. As of today, disruptions of a few acrosomal enzymes are reported, but defects in sperm fertilizing ability is not reported *in vivo* [15,19]. However, as indicated in the present paper, active protease(s) exist inside acrosome. This suggests that a processing of some membrane proteins during epididymal maturation is essential for fertilization.

Subcellular localization and function of unglycosylated IZUMO

In virus, if the fusion (F) proteins are unglycosylated by mutation, it is reported to be transported to the cell surface and consequently not able to mediate cell–cell fusion [20,21]. However, unglycosylated IZUMO was transported to its proper location and spread to the entire head surface after acrosome reaction as in the normal IZUMO, indicating the glycosylation of IZUMO is not essential for proper protein trafficking in sperm.

It was clear that N204Q-IZUMO could rescue the sterile male to fertile without the aid of glycosylation of IZUMO (Fig. 1A). This indicates that the glycosylation is not "essential" for fusion. However, the N204Q-IZUMO rescue was not as effective as wild-type IZUMO rescue. We think there are three possible explanations for the inefficient rescue: (i) the lack of glycosylation decreased the fusion-facilitating ability of IZUMO, (ii) the disappearance of glycan in IZUMO evoked the fragmentation system and only a small amount of IZUMO was retained on sperm, (iii) a mixture of (i) and (ii).

Numerous glycoproteins have been proven to be involved in sperm–egg interaction. [6,10]. However, the role of their glycan moiety remains unclear. Using the gene disruption and its rescue by mutant proteins, we could demonstrate that at least one of the roles of *N*-glycan in IZUMO is to protect IZUMO from fragmentation during sperm maturation in epididymis. As far as we searched, this is the first *in vivo* indication of glycans proteolytic fragmentation protecting activity.

Acknowledgments

We thank Akiko Kawai, Yumiko Koreeda and Yoko Esaki for technical assistance with producing transgenic mouse lines. This work was supported by grants from the Ministry of Education, Culture, Sports, Science, and Technology of Japan, the 21st Century 200 COE program from the Ministry of Education, Culture, Sports, Science, and Technology of Japan, The Nakajima foundation, The Uehara memorial foundation, NOVARTIS Foundation (Japan) for the Promotion of Science, and The Senri life science foundation.

References

[1] K. Ohtsubo, J.D. Marth, Glycosylation in cellular mechanisms of health and disease, Cell 126 (2006) 855–867.
[2] T.O. Akama, H. Nakagawa, K. Sugihara, S. Narisawa, C. Ohyama, S. Nishimura, D.A. O'Brien, K.W. Moremen, J.L. Millan, M.N. Fukuda, Germ cell survival through carbohydrate-mediated interaction with Sertoli cells, Science 295 (2002) 124–127 (New York, NY).
[3] R. Yamaguchi, K. Yamagata, M. Ikawa, S.B. Moss, M. Okabe, Aberrant distribution of ADAM3 in sperm from both angiotensin-converting enzyme (Ace)- and calmegin (Clgn)-deficient mice, Biol. Reprod. 75 (2006) 760–766.
[4] M. Ikawa, T. Nakanishi, S. Yamada, I. Wada, K. Kominami, H. Tanaka, M. Nozaki, Y. Nishimune, M. Okabe, Calmegin is required for fertilin α/β heterodimerization and sperm fertility, Dev. Biol. 240 (2001) 254–261.
[5] M. Ikawa, I. Wada, K. Kominami, D. Watanabe, K. Toshimori, Y. Nishimune, M. Okabe, The putative chaperone calmegin is required for sperm fertility, Nature 387 (1997) 607–611.
[6] H.M. Florman, P.M. Wassarman, *O*-linked oligosaccharides of mouse egg ZP3 account for its sperm receptor activity, Cell 41 (1985) 313–324.
[7] T.L. Rankin, Z.B. Tong, P.E. Castle, E. Lee, R. Gore-Langton, L.M. Nelson, J. Dean, Human ZP3 restores fertility in Zp3 null mice without affecting order-specific sperm binding, Development 125 (1998) 2415–2424 (Cambridge, England).
[8] R.H. Ponce, U.A. Urch, R. Yanagimachi, Inhibition of sperm-egg fusion in the hamster and mouse by carbohydrates, Zygote 2 (1994) 253–262 (Cambridge, England).
[9] N. Inoue, M. Ikawa, A. Isotani, M. Okabe, The immunoglobulin superfamily protein Izumo is required for sperm to fuse with eggs, Nature 434 (2005) 234–238.
[10] N. Inoue, M. Ikawa, T. Nakanishi, M. Matsumoto, M. Nomura, T. Seya, M. Okabe, Disruption of mouse CD46 causes an accelerated spontaneous acrosome reaction in sperm, Mol. Cell. Biol. 23 (2003) 2614–2622.
[11] K. Yamagata, T. Nakanishi, M. Ikawa, R. Yamaguchi, S.B. Moss, M. Okabe, Sperm from the calmegin-deficient mouse have normal abilities for binding and fusion to the egg plasma membrane, Dev. Biol. 250 (2002) 348–357.
[12] S. Metayer, F. Dacheux, J.L. Dacheux, J.L. Gatti, Germinal angiotensin I-converting enzyme is totally shed from the rodent sperm membrane during epididymal maturation, Biol. Reprod. 67 (2002) 1763–1767.
[13] J.R. Hagaman, J.S. Moyer, E.S. Bachman, M. Sibony, P.L. Magyar, J.E. Welch, O. Smithies, J.H. Krege, D.A. O'Brien, Angiotensin-converting enzyme and male fertility, in: Proceedings of the National Academy of Sciences of the United States of America, 95, 1998, pp. 2552–2557.
[14] N. Kohno, K. Yamagata, S. Yamada, S. Kashiwabara, Y. Sakai, T. Baba, Two novel testicular serine proteases, TESP1 and TESP2, are present in the mouse sperm acrosome, Biochem. Biophys. Res. Commun. 245 (1998) 658–665.
[15] T. Baba, S. Azuma, S. Kashiwabara, Y. Toyoda, Sperm from mice carrying a targeted mutation of the acrosin gene can penetrate the oocyte zona pellucida and effect fertilization, J. Biol. Chem. 269 (1994) 31845–31849.
[16] A. Honda, K. Yamagata, S. Sugiura, K. Watanabe, T. Baba, A mouse serine protease TESP5 is selectively included into lipid rafts of sperm membrane presumably as a glycosylphosphatidylinositol-anchored protein, J. Biol. Chem. 277 (2002) 16976–16984.
[17] K. Ohmura, N. Kohno, Y. Kobayashi, K. Yamagata, S. Sato, S. Kashiwabara, T. Baba, A homologue of pancreatic trypsin is localized in the acrosome of mammalian sperm and is released during acrosome reaction, J. Biol. Chem. 274 (1999) 29426–29432.
[18] T. Nakanishi, M. Ikawa, S. Yamada, K. Toshimori, M. Okabe, Alkalinization of acrosome measured by GFP as a pH indicator and its relation to sperm capacitation, Dev. Biol. 237 (2001) 222–231.
[19] M. Yamashita, A. Honda, A. Ogura, S.I. Kashiwabara, K. Fukami, T. Baba, Reduced fertility of mouse epididymal sperm lacking Prss21/Tesp5 is rescued by sperm exposure to uterine microenvironment, Genes Cells 10 (2008) 1001–1013.
[20] G. Zimmer, I. Trotz, G. Herrler, *N*-glycans of F protein differentially affect fusion activity of human respiratory syncytial virus, J. Virol. 75 (2001) 4744–4751.
[21] H.C. Aguilar, K.A. Matreyek, C.M. Filone, S.T. Hashimi, E.L. Levroney, O.A. Negrete, A. Bertolotti-Ciarlet, D.Y. Choi, I. McHardy, J.A. Fulcher, S.V. Su, M.C. Wolf, L. Kohatsu, L.G. Baum, B. Lee, *N*-glycans on Nipah virus fusion protein protect against neutralization but reduce membrane fusion and viral entry, J. Virol. 80 (2006) 4878–4889.

Cd52, known as a major maturation-associated sperm membrane antigen secreted from the epididymis, is not required for fertilization in the mouse

Ryo Yamaguchi[1,2], Kazuo Yamagata[3], Hidetoshi Hasuwa[1], Emiko Inano[1], Masahito Ikawa[1] and Masaru Okabe[1,2,*]

[1]*Research Institute for Microbial Diseases, and*
[2]*Pharmaceutical Sciences, Osaka University, Osaka 565-0871, Japan*
[3]*Laboratory for Genomic Reprogramming, RIKEN, Center for Developmental Biology, Kobe 650-0047, Japan*

CD52 is a glycosylphosphatidylinositol (GPI)-anchored antigen expressed on lymphocytes and in epididymal epithelial cells. CD52 is also known as "maturation-associated sperm antigen" but its function is unknown. We therefore generated *Cd52* disrupted mice. The resulting *Cd52* null mice were healthy, even though *Cd52* is expressed on cells of the immune system. We then examined a possible role for CD52 in reproduction. Sperm from *Cd52*-deficient males were investigated and the viability, motility, morphology, and incidence of spontaneous acrosome reactions were found to be all similar to values for wild-type sperm. In *in vitro* fertilization system, the sperm showed normal fertilizing ability. As CD52 was found to be transferred onto sperm only after they had migrated into the vas deferens, we examined the behavior of sperm from *Cd52*-deficient mice *in vivo*. The mice mated naturally and we observed that a normal number of sperm passed through the uterotubal junction, known to the crucial hurdle for various gene knockouts resulting in infertile sperm. As a consequence, there was no difference in the litter size from the wild-type and *Cd52*-null males. Our results therefore indicate CD52 is not required for fertilization in the mouse either *in vivo* or *in vitro*.

Introduction

Sperm are produced from spermatogonial cells as a highly differentiated cell to fertilize eggs but they have no fertilizing ability when they leave testis. Sperm require a maturation process during passage through epididymis. For example, swimming ability and egg interacting ability of sperm are reported to be acquired during the maturation step (Cooper 1995; Toshimori 2003). The ability of sperm to undergo the acrosome reaction, a prerequisite for sperm to fertilize eggs, is also known to increase during the epididymal maturation (Williams *et al.* 1991). This sperm maturation process is associated with reorganization of membrane structures such as processing of membrane proteins on sperm surface (Kim *et al.* 2006), changes in plasma membrane phospholipids composition (Sullivan *et al.* 2005), and the accumulation or modification of glycoproteins on sperm surface (Kirchhoff 1996; Tulsiani 2006). Various glycoproteins are known to be secreted from the epithelial cells of male reproductive tract and transferred on sperm during epididymal passage (Cornwall *et al.* 1990; Vreeburg *et al.* 1990; Sullivan *et al.* 2005; Busso *et al.* 2007). Thus these glycoproteins may function as a primary interface between sperm and female reproductive tract and eggs.

A highly sialylated glycosylphosphatidylinositol (GPI)-anchored protein CD52 initially found on lymphocytes is also known as SAGA-1, GP20, Cambridge pathology 1 antigen and epididymal secretory protein E5. It is one of the few well-defined antigens secreted from the epididymal cells, is transferred to the sperm plasma membrane during epididymal passage, and alters the characteristics of sperm surface. CD52 is exposed in the equatorial region of the sperm head at the end of the capacitation process in human (Yeung *et al.* 2001). Both CD52 on sperm and lymphocyte share the same peptide sequence but carbohydrate moiety is different in these two cases. Thus, CD52 on sperm could be antigenic to females. Actually, anti-CD52 mab (MAb H6-3C4) is generated from an infertile woman's peripheral

Communicated by: Takeo Kishimoto
**Correspondence*: okabe@gen-info.osaka-u.ac.jp

DOI: 10.1111/j.1365-2443.2008.01210.x

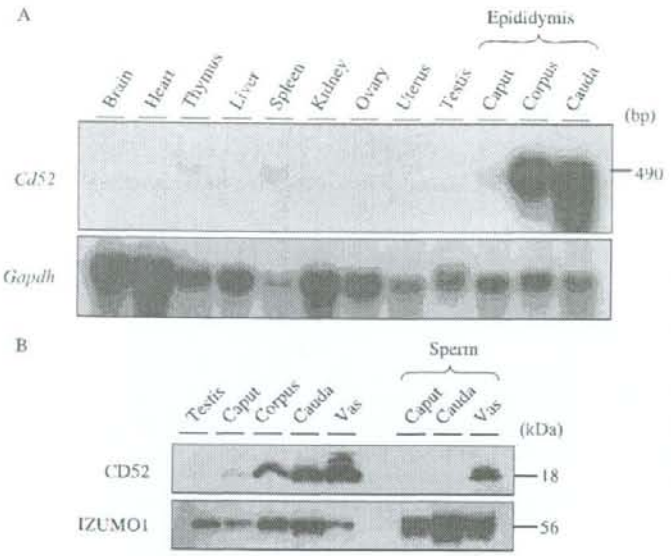

Figure 1 Tissue distribution of *Cd52* mRNA and protein. (A) Northern blot containing equal amounts of total RNA (10 μg) was hybridized with ^{32}P-dCTP labeled cDNA fragments of *Cd52* and *Gapdh*. (B) Testes, male reproductive ducts and sperm protein were extracted with lysis buffer containing Triton X-100 and subjected to immunoblot analysis. Western blots containing equal amounts of tissue proteins (30 μg) and sperm protein (10 μg) were hybridized with anti-CD52 polyclonal antibody. For control sperm protein, mouse IZUMO1 was detected with anti-IZUMO1 monoclonal antibody (#125).

blood lymphocytes. The antibody was shown to have a strong complement-dependent, sperm-immobilizing activity, which indicates the possibility of CD52 being a candidate contraceptive target molecule. Although a clear implication of CD52 in fertilization mechanism is not reported, the covering of sperm membrane with CD52 might have an effect on the sperm-egg, or sperm-female reproductive tract interactions (such as storage of spermatozoa in the caudal part of the isthmus, in tight contact with the epithelium cells lining the oviduct (Topfer-Petersen 1999)).

In the study of mechanism of fertilization, many factors are designated as "important" factors from the experiments in which antibodies and ligands added to *in vitro* fertilization system showed inhibitory activities. However, many such discovered factors turned out to be "not essential" by gene disruption, suggesting that conclusive demonstrations of the protein functions become more reliable from the observation of the gene disrupted animals. Therefore, we tried to disrupt CD52 gene to examine its role in fertilization.

Results

Expression of Cd52 in various organs (Northern and Western blotting)

Cd52 is known to be expressed in thymus and in spleen (Kubota *et al.* 1990). The anti-CD52 monoclonal antibodies are used as one of the treatments to prevent the rejection of transplanted organs (Calne *et al.* 1999; Hale *et al.* 2000). However, the expression levels of *Cd52* were much higher in epididymal tissues than in those immunity-related organs (Fig. 1A). It has been reported that the human CD52 is secreted from the male reproductive tract and is bound to the sperm surface (Kirchhoff 1996). When we examined the presence of CD52 in the mouse using Western blotting, CD52 was not found in the caput epididymis but substantial amounts of CD52 were found starting from the corpus epididymal section to vas deferens. Interestingly, CD52-positive sperm (examined by Western blotting) were only found in the vas deferens (Fig. 1B).

Immunohistochemistry

The localization of CD52 was examined by immunostaining. We detected almost no staining in caput epididymal sections, but the epithelial cells of the cauda epididymal sections showed an intense staining (Fig. 2). In the vas deferens, an equally strong staining was observed in the epithelial cells, but different from epididymis, the staining was spread to the ductal area of the vas deferens. This staining was not a nonspecific binding, because no staining was observed in *Cd52*$^{-/-}$ mice.

While sperm from cauda epididymis showed no reactivity to anti-CD52 antibody, approximately 25% of sperm population from vas deferens was stained by anti-CD52 antibody (Fig. 3C). The staining pattern of CD52 was spotty and was basically localized in the midpiece area and

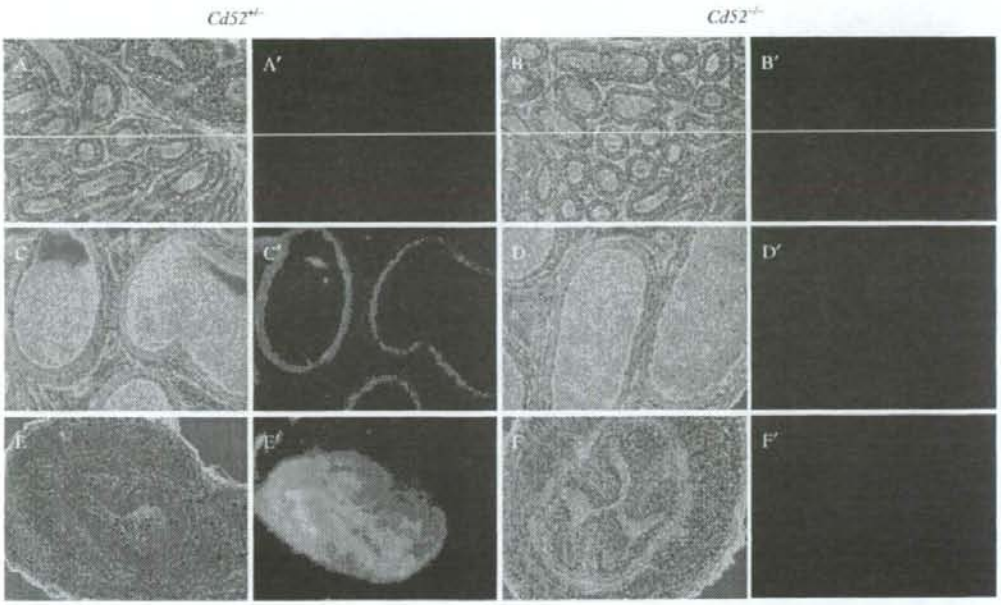

Figure 2 Expression of CD52 in epididymis and vas deferens. The sections of caput epididymis (A, B), cauda epididymis (C, D), and vas deferens (E, F) were subjected to indirect immunofluorescence employing anti-CD52 monoclonal antibody followed by Alexa Flour 488-conjugated anti-rat second antibody. Immunoreactivity was visualized with fluorescent microscopy. CD52 protein was only detected in the cauda epididymis and vas deferens from heterozygous mouse (C, E, and G). No fluorescence was detected in the tissues from *Cd52*-deficient mice (B, D, and F).

sometimes extended to the head regions. Ejaculated sperm recovered from the uterus within 1 h after plug formation showed a similar spotty staining pattern as sperm from vas deferens shown in Fig. 3E, indicating that the encounter of sperm with accessory gland secretions at ejaculation seems not to affect the localization of CD52 on sperm. Together with the result of Western and Northern blotting experiments, it was indicated that CD52 is secreted from the epithelial wall and binds to the sperm in the vas deferens in mouse.

Generation of Cd52-deficient mice

In order to examine the roles of CD52, we disrupted the *Cd52* gene by homologous recombination. The mouse *Cd52* gene consists of two exons and is mapped to chromosome 4 (Tone *et al.* 1999). The targeting vector was designed to remove both exons of *Cd52* (Fig. 4A) and was electroporated into D3 ES cells after linearization. Potentially targeted ES cell clones were separated by positive–negative selection with G418 and acyclovir. Correct targeting of the *Cd52* allele in ES cell clones was determined by PCR for homologous recombination on both ends (Fig. 4B). Mating between heterozygous mutant mice yielded the expected Mendelian ratios: $Cd52^{+/+}$, 26%; $Cd52^{+/-}$, 52%; $Cd52^{-/-}$, 22% of offspring ($n = 116$). Northern and Western blot analysis showed that *Cd52* mRNA expression was undetectable in the $Cd52^{-/-}$ epididymis (Fig. 4C). CD52 protein was also not detected in sperm from the vas deferens in $Cd52^{-/-}$ mice (Fig. 4D). $Cd52^{-/-}$ mice exhibited normal development and grew up as healthy adults with normal CD4/CD8 positive cell ratios (Fig. S1 in Supplementary Material). We do not exclude the possibility that we overlooked the phenotype, but the chance is high that the role of CD52 in immune system is masked by some compensating factors or the role is not essential in lymphocytes and in splenocytes.

Fertility of sperm in CD52 null epididymis

CD52 expressed in epididymis may contribute to supporting epididymal function *per se* in nursing sperm. We collected and observed the motility of epididymal sperm from $Cd52^{-/-}$ male mice using automated sperm analyzer

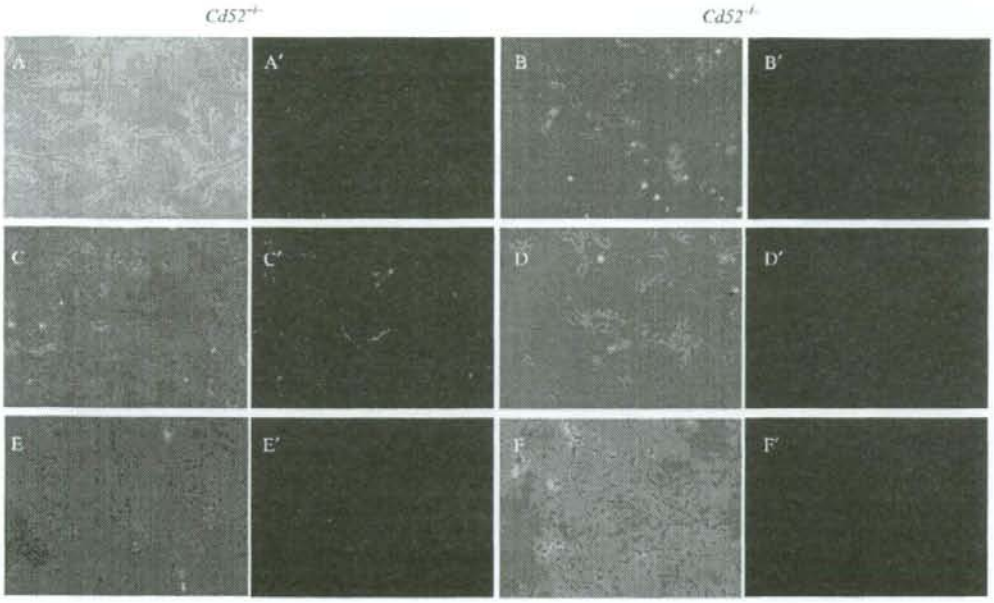

Figure 3 Immunolocalization of CD52 protein on mouse sperm. Sperm from cauda epididymis (A, B), vas deferens (C, D) and recovered from uterus (E, F) were immunostained with anti-CD52 monoclonal antibody combined with Alexa Flour 488-conjugated second antibody. Immunoreactivity was visualized with fluorescent microscopy (×400). No fluorescence was detected on sperm from the cauda epididymis (A) and on *Cd52*-deficient sperm (B, D, and F).

SMAS. No difference in the motility or the swimming pattern was found compared to sperm from wild-type mice (Table 1 & Fig. 5). Using the double transgenic mouse line, CD52 KO bearing *Acr-EGFP* transgene, we examined the effect of CD52 disruption on the spontaneous acrosome reaction of sperm from cauda epididymis and from vas deferens by a flow cytometer. Sperm from *Cd52*$^{-/-}$ male showed no significant difference from those from control male, even sperm from the cauda epididymis and vas deferens (Fig. 6). The ionophore induced acrosome reaction which was caused by the addition of A23187 was also found not to be affected by the CD52 disruption (data not shown). To confirm the fact that sperm maturation in epididymis was normal in CD52 null mice, *in vitro* fertilization assay was performed using sperm from CD52 −/−, +/−, and +/+ mice and it resulted in a similar fertilization ratio as expected (Table 2).

Fertility of ejaculated sperm in CD52 null mice

Usually, cauda epididymal sperm are used for *in vitro* fertilization experiments. However, this sperm population is not yet covered with CD52 (Fig. 3), indicating that mouse epididymal sperm are competent to bind and penetrate eggs without having CD52 on their surface. Therefore, if CD52 functions in fertilization, it might be through a characteristic step involved in *in vivo* fertilization processes, such as ejaculated sperm moving up the female reproductive tract to where fertilization takes place.

To clarify the role of CD52 in fertilization *in vivo*, we mated *Cd52*$^{-/-}$ male mice with superovulated wild-type female mice. Two hours after coitus, whole mount sections of oviducts were made and serial sections were observed by bright field microscopy. Close examination of sections of the uterotubal junction revealed that sperm derived from both CD52 +/+ and −/− sperm had migrated through the ostium of the colliculus tubarius, and were found inside the oviduct (Fig. 7).

There was no difference in the mating ratio and fertility compared to wild-type mice (Table 3). In natural mating, the number of pups sired by wild-type and *Cd52*$^{-/-}$ male mice were similar (control, 9.55 ± 1.70, $n = 18$; homozygous, 9.14 ± 1.02, $n = 14$), coinciding with the result of migrating equal number of sperm into the oviduct. Thus the disruption experiment revealed that CD52 is "dispensable" in fertilization.

Table 1 Comparison of sperm motility prepared from CD52 +/+, +/−, and −/− mice

Parameters	Incubation time (min)	+/+	+/−	−/−
Percentage of motile spermatozoa (%)	15	76.1 ± 10.8	82.7 ± 8.4	76.3 ± 2.6
	60	72.7 ± 11.1	73.1 ± 7.1	67.2 ± 4.8
	120	72.4 ± 6.9	70.4 ± 16.8	64.2 ± 3.9
Straight line velocity (μm/s)	15	108.6 ± 16.9	99.7 ± 8.0	104.4 ± 15.7
	60	74.3 ± 18.7	90.5 ± 16.2	97.3 ± 6.1
	120	73.8 ± 17.7	72.6 ± 10.6	83.4 ± 19.4
Curvilinear (μm/s)	15	306.1 ± 17.2	291.0 ± 17.1	279.4 ± 31.0
	60	289.9 ± 42.9	305.8 ± 28.7	312.2 ± 20.8
	120	273.4 ± 63.5	276.2 ± 31.1	306.9 ± 47.5
Linearity	15	0.37 ± 0.039	0.35 ± 0.029	0.38 ± 0.026
	60	0.27 ± 0.077	0.31 ± 0.027	0.32 ± 0.014
	120	0.28 ± 0.013	0.27 ± 0.019	0.27 ± 0.025
Amplitude of lateral head displacement (μm)	15	9.0 ± 0.7	8.2 ± 0.23	7.9 ± 1.06
	60	8.5 ± 1.0	8.5 ± 0.39	9.0 ± 1.01
	120	7.9 ± 0.7	7.3 ± 0.80	8.9 ± 1.18

The data represent the means ± SD of three independent experiments.

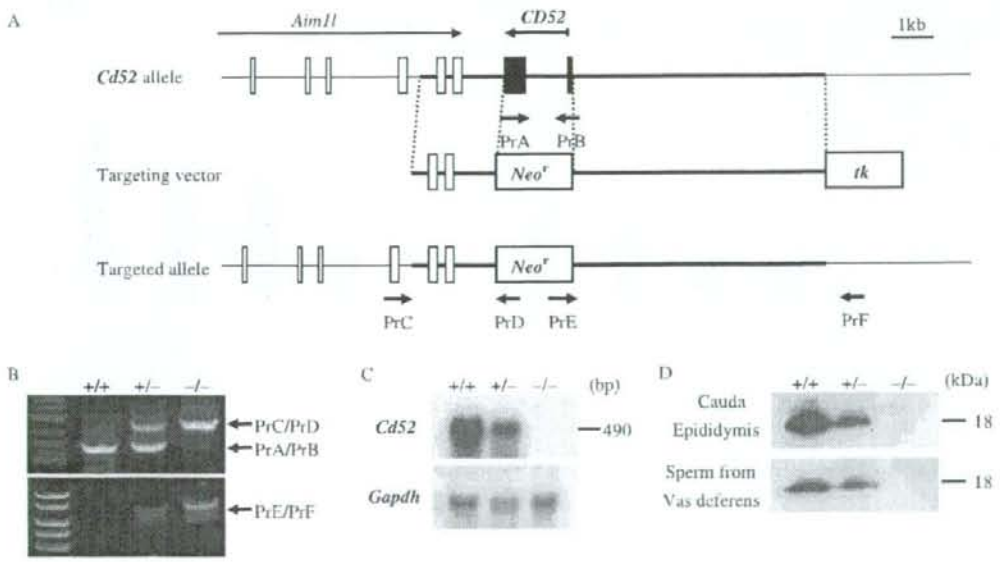

Figure 4 Production of *Cd52*-deficient mice. For the targeted disruption of mouse Cd52 allele, all two exons encoding mouse CD52 protein (closed boxes) was replaced by the neomycin-resistant-cassette (*Neo*^{r}). A herpes simplex virus thymidine kinase gene (*tk*) was introduced into the targeting construct for negative selection. (B) Genotyping of tail tip DNA by PCR amplification with primers indicated in the figure. (C) Northern blot analysis of total RNA from *Cd52*$^{+/+}$ (+/+), *Cd52*$^{+/-}$ (+/−), and *Cd52*$^{-/-}$ (−/−) cauda epididymis. Blots were hybridized with ^{32}P-dCTP labeled cDNA fragments of *Cd52* and *Gapdh*. (D) Western blot analysis of cauda epididymal lysate and sperm lysate in vas deferens from *Cd52*$^{+/+}$ (+/+), *Cd52*$^{+/-}$ (+/−), and *Cd52*$^{-/-}$ (−/−) mice.

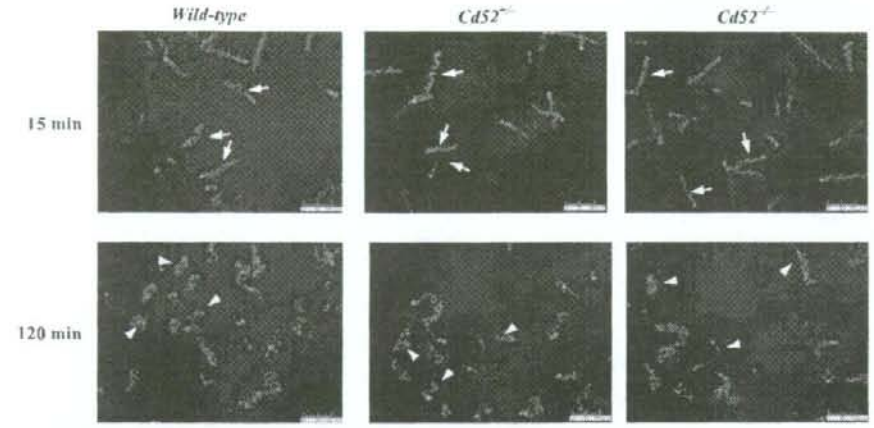

Figure 5 A change in swimming patterns of sperm during incubation in TYH medium. Sperm from CD52 +/− and −/− mice were incubated in TYH medium and analyzed by the computer-aided Sperm Motility Analysis System (SMAS). Almost all the sperm showed straightforward movement at 15 min of incubation (arrows), but a comparable number of characteristic hyperactivated movements (arrowheads) appeared in the sperm population after 120 min of incubation both in sperm from CD52 +/− and −/− mouse lines.

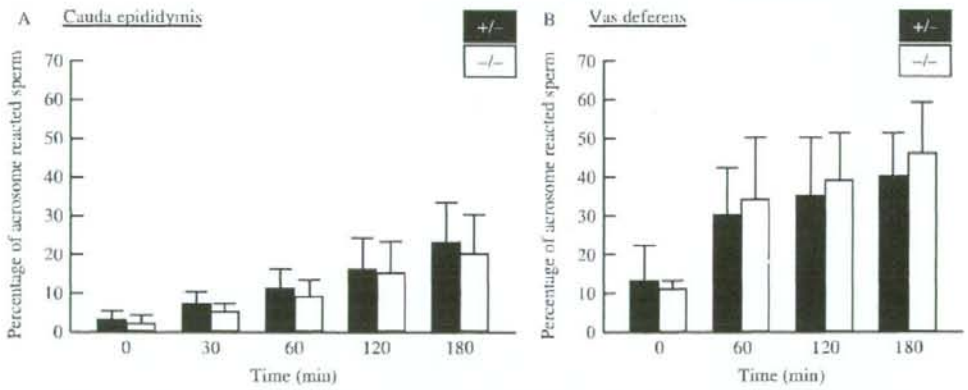

Figure 6 Time course of the acrosome reaction in *Cd52*$^{-/-}$ mice. Mice with the *Cd52*$^{+/-}$ allele were bred with a green sperm transgenic mouse line and a double-transgenic mouse line, *Cd52*$^{-/-}$ mice with green sperm was obtained. Sperm from cauda epididymis (A) and vas deferens (B) from this double-transgenic mouse line were incubated in TYH medium and analyzed for their acrosomal integrity by flow cytometry. Sperm from *Cd52*$^{+/-}$ (closed column) and *Cd52*$^{-/-}$ (open column) littermate mice were compared. Error bars represent mean ± SDs from seven (cauda epididymis) or four (vas deferens) independent experiments.

Discussion

In the process of studying fertilization, various antibodies to sperm were produced in the past. The clarification of the antigens and subsequent disruptions of the corresponding genes indicated various antigens to be essential (ADAM2, ADAM1a, ADAM3, ACE, and IZUMO1). On the other hand, many factors turned out to be "not essential" (acrosin, CD46, PH20, ADAM1b, GalTase etc.) for fertilization (see review, Okabe & Cummins (2007)). These data suggest that we have to be careful when we examine the roles of a certain factor in fertilization using antibodies and/or ligands. The gene disruption experiment is a time-consuming effort but could often provide clear understanding which is not possible to obtain with normal biochemical and/or physiological analysis.